表4 欧米諸国におけるIPVを用いた定期接種スケジュール（文献10)～13)より引用，作成）

国名	IPVの接種回数と時期							
米国	①（2カ月）	②（4カ月）	③（6～18カ月）	④（4～6歳）				
カナダ	①（2カ月）	②（4カ月）	③（6カ月）	④（12～18カ月）	⑤（4～6歳）			
英国	①（2カ月）	②（3カ月）	③（4カ月）		④（3～5歳）		⑤（13～18歳）	
フランス	①（2カ月）	②（3カ月）	③（4カ月）	④（12～18カ月）	⑤（6歳）	⑥（11歳）	⑦（16歳）	
スウェーデン		①（3カ月）	②（5カ月）	③（12カ月）	④（6歳）			
オランダ		①（3カ月）	②（4カ月）	③（5カ月）	④（12カ月）	⑤（4歳）	⑥（9歳）	

イルスが不活化されているIPVは，免疫不全宿主に接種した場合このような副反応の懸念がない．ただし，免疫原性が健常児と比べると劣る可能性はある．

3．接種スケジュール

IPVは，生後2カ月から接種が可能である．1～2カ月間隔で計2～3回の初期免疫を行い，6～12カ月後の追加免疫により基礎免疫が完了する．小学校就学前に，再度追加接種を実施する場合も多い．各国がIPVを用いて実施している定期接種スケジュールの例を**表4**[10)～13)]に示した．

注射製剤であるIPVは，DPT，B型肝炎，Hibなどとの混合ワクチンとして，欧米では使用されている．簡便さの点からは経口投与のOPVに及ばないが，他のワクチンとの混合製剤を用いて，一度で多種類の疾患に対する免疫を付与できることはメリットである（**表1**）．

わが国における今後のIPV

OPVの成分である弱毒Sabin株から製造されるIPVがわが国で開発され，DPTとの混合製剤を用いた臨床試験が実施されている．ポリオ強毒野生株を用いる海外のIPVと比較して，製造施設の安全管理やバイオセイフティの面からも注目される．一方，海外ですでに使用経験が豊富な野生強毒ポリオウイルス由来株を用いたIPVやDPTとの混合製剤も臨床試験が進行中である．

VAPPのリスクを考慮し，国内では未承認の海外IPVを輸入して使用する動きが活発化している．現行の定期接種で用いられるOPVを一刻も早くIPVに変更したいという思いは多くの者が一致するところであろうが，国内未承認製剤の使用には問題がつきまとう．乳児期は重症感染症や乳幼児突然死症候群の好発期であり，偶発例も含めればワクチン接種後10万～数百万例に1例程度は突然死がおこりうる[14)]．予防接種後に健康被害が発生した場合，接種したワクチンと因果関係がなくても，その発生のタイミングなどで副反応を完全に否定することができなければ，接種した側・された側ともワクチンの関与に対する不信感や法律的対処への対応に戸惑うことは多い．未承認ワクチン接種後にそのような状況に遭遇すれば，さらに不幸な状況に陥ることが懸念される．国内未承認ワクチンを使用するにあたっては，「法律で認められた薬剤を使用することにより，被接種者・医師双方ともいろいろな観点で保護されていること」と，「未承認薬剤を使用する際には，その保護のほとんどは適用が期待できないこと」を被接種者・医師ともに十分認識しておくことが必要である．

文 献

1) 萩原昭夫：エンテロウイルス感染症．臨床とウイルス 23 (Suppl)：156-163，1995
2) 中野貴司：ポリオ．日本小児感染症学会・編，改訂第3版 日常診療に役立つ小児感染症マニュアル2011．東京医学社，東京，482-489，2011
3) Sutter RW, Kew OM, Cochi SL: Poliovirus vaccine-live. Plotkin SA, Orenstein WA, Offit PA eds., Vaccines 5th ed., WB Saunders, Philadelphia, 631-685, 2008
4) Bosley ARJ, Speirs G, Markham NI: Provocation poliomyelitis: vaccine associated paralytic poliomyelitis related to a rectal abscess in an infant. J Infect 47: 82-84, 2003
5) 財団法人日本ポリオ研究所：経口生ポリオワクチン（セービン）Ⅰ・Ⅱ・Ⅲ型混合 添付文書．2009年9月改訂（第6版）
6) 厚生労働省：ポリオとポリオワクチンの基礎知識．2011年10月4日版
http://www.mhlw.go.jp/bunya/kenkou/polio/qa.html
7) 国立感染症研究所：世界のワクチン株由来ポリオウイルス（VDPVs）－2006年1月～2007年8月におけるアップデート．病原微生物検出情報 IASR 28: 328-329，2007
8) Nakano T: Japanese vaccinations and practices, with particular attention to polio and pertussis. Trav Med Infect Dis 9: 169-175, 2011
9) 中野貴司：ポリオワクチンの光と影－根絶計画そしてワクチン関連麻痺－．小児科臨床 64: 1739-1745，2011
10) Plotkin SA, Vidor E: Poliovirus vaccine-inactivated. Plotkin SA, Orenstein WA, Offit PA eds., Vaccines 5th ed., WB Saunders, Philadelphia, 605-629, 2008
11) 中野貴司：不活化ポリオワクチン．小児科診療 72: 2297-2301，2009
12) CDC: Recommended Child hood and Adolescent Immunization Schedule, USA
http://www.cdc.gov/vaccines/recs/schedules/child-schedule.htm
13) NHS: National Health Service, UK
http://www.immunisation.nhs.uk/Immunisation_Schedule
14) 厚生労働省医薬品等安全対策部会安全対策調査会，子宮頸がん等ワクチン予防接種後副反応検討会：小児用肺炎球菌ワクチン，ヒブワクチンの安全性の評価結果について．2010年3月24日

著者連絡先
〒700-8505 岡山県岡山市北区中山下2-1-80
川崎医科大学小児科
中野貴司

Journal of General Virology (2011), **92**, 287–291 DOI 10.1099/vir.0.022418-0

Short Communication

Adaptive mutations in the genomes of enterovirus 71 strains following infection of mouse cells expressing human P-selectin glycoprotein ligand-1

Kohei Miyamura,[1,2] Yorihiro Nishimura,[1] Masahiro Abo,[2] Takaji Wakita[1] and Hiroyuki Shimizu[1]

Correspondence
Hiroyuki Shimizu
hshimizu@nih.go.jp

[1]Department of Virology II, National Institute of Infectious Diseases, 4-7-1 Gakuen, Musashimurayama-shi, Tokyo 208-0011, Japan

[2]Department of Rehabilitation Medicine, Jikei University School of Medicine, 3-19-18 Nishishinbashi, Minato-ku, Tokyo 105-8471, Japan

We recently identified human P-selectin glycoprotein ligand-1 (PSGL-1) as a functional enterovirus 71 (EV71) receptor and demonstrated PSGL-1-dependent replication for some EV71 strains in human leukocytes. Here, we report that four out of five PSGL-1-binding strains of EV71 replicated poorly in mouse L929 cells stably expressing human PSGL-1 (L-PSGL-1 cells). Therefore, we compared the replication kinetics and entire genomic sequence of five original EV71 strains and the corresponding EV71 variants (EV71-LPS), which were propagated once in L-PSGL-1 cells. Direct sequence comparison of the entire genome of the original EV71 strains and EV71-LPS variants identified several possible adaptive mutations during the course of replication in L-PSGL-1 cells, including a putative determinant of the adaptive phenotype in L-PSGL-1 cells at VP2-149. The results suggest that an adaptive mutation, along with a PSGL-1-binding phenotype, may facilitate efficient PSGL-1-dependent replication of the EV71 strains in L-PSGL-1 cells.

Received 28 March 2010
Accepted 13 October 2010

Enterovirus 71 (EV71) is a small non-enveloped virus with a ssRNA genome of about 7500 nt, and is a major causative agent of hand, foot, and mouth disease. Hand, foot, and mouth disease is usually a mild and self-limiting febrile disease in children, but EV71 infection has been associated with various neurological diseases such as aseptic meningitis, polio-like paralysis and acute encephalitis with neurological pulmonary oedema, mainly in young children and infants (Chan *et al.*, 2000; Ho *et al.*, 1999; McMinn, 2002). Recently, EV71 outbreaks with a number of fatal cases have been reported throughout the world, particularly in the Asia–Pacific region, and the activity of EV71 infection remains a major public health threat (Yang *et al.*, 2009). Despite the importance of EV71, little is known about the pathogenesis of severe neurological diseases associated with EV71 at the molecular level.

Recently, we demonstrated that human P-selectin glycoprotein ligand-1 (PSGL-1) is one of the functional receptors for EV71 (Nishimura *et al.*, 2009). PSGL-1 is a type I sialomucin membrane protein expressed mainly on leukocytes (Laszik *et al.*, 1996; Sako *et al.*, 1993). PSGL-1 on leukocytes binds to selectins on the endothelium with high affinity, and the interaction between PSGL-1 and selectins mediates leukocyte rolling during the initial stage of inflammatory cell recruitment to inflamed tissues. On the other hand, Yamayoshi *et al.* (2009) identified scavenger receptor class B member (SCARB2) as another functional cellular receptor for EV71. SCARB2 is a type III transmembrane protein with double-membrane anchoring and cytoplasmic domains at N and C termini (Eskelinen *et al.*, 2003). Like the expression of PSGL-1, human SCARB2 expression enables normally non-susceptible mouse L929 cells to support viral replication and development of EV71 induced cytopathic effects (CPE) (Yamayoshi *et al.*, 2009). All EV71 strains and the prototype strain (G-10) of coxsackievirus A16 replicate in L929 cells expressing human SCARB2 and in SCARB2-positive RD cells in a SCARB2-dependent manner (Yamayoshi *et al.*, 2009). Previously examined EV71 strains can be classified as PSGL-1-binding and PSGL-1-non-binding strain (Nishimura *et al.*, 2009).

To investigate the replication of various PSGL-1-binding strains of EV71 in more detail, we established a mouse L929 cell line that highly and stably expresses human PSGL-1 on the cell surface (L-PSGL-1 cells) (Nishimura *et al.*, 2009). In the present study, we have shown that a single passage of the original EV71 strains in L-PSGL-1 cells induced one or more amino acid substitutions

The GenBank/EMBL/DDBJ accession numbers for the sequences reported in this paper are AB550332–AB550341.

Supplementary figures are available with the online version of this paper.

encoded in the EV71 genome, which may be associated with the adaptive phenotype in these cells, and that the substitution at VP2-K149I/M may be especially important.

We examined whether five PSGL-1-binding strains of EV71 (Table 1) induced CPE in L-PSGL-1 cells. The cells in 24-well tissue culture trays (1×10^5 cells) were infected with EV71 [1×10^6 50 % cell culture infectious dose ($CCID_{50}$)] for 1 h at 34 °C. The cells were washed and cultured for 4 days at 34 °C. L-PSGL-1 cells exhibited CPE 4 days after infection with the 1095 strain as reported previously (data not shown) (Nishimura *et al.*, 2009). However, four other strains (75-Yamagata, SK-EV006, C7/Osaka and KED005) did not induce significant CPE 4 days post-infection (data not shown). Because we could immunofluorescently detect a few cells that expressed the EV71 antigen in infected L-PSGL-1 cells (data not shown), we attempted to propagate original EV71 in L-PSGL-1 cells. The preparation of L-PSGL-1-adapted EV71 variants (EV71-LPS) is summarized in Supplementary Fig. S1 (available in JGV Online). L-PSGL-1 cells (1×10^6 cells) were inoculated with original EV71 (1×10^7 $CCID_{50}$) for 1 h at 34 °C in a 10 cm dish. Inoculated cells were then washed three times and incubated in 10 ml medium at 34 °C. We incubated the L-PSGL-1 cells until almost all cells showed CPE (about 10 days). Finally, we harvested the virus in the culture supernatant and named it EV71-LPS. When we infected L-PSGL-1 cells with EV71-LPS, all EV71 variants induced apparent CPE within 4 days after inoculation (data not shown). VP1 antigens were also detected in L-PSGL-1 cells infected with all EV71-LPS variants (data not shown). These observations indicated that EV71-LPS replicated well in L-PSGL-1 cells.

Next, we infected L-PSGL-1 cells with EV71-LPS in the presence of anti-human PSGL-1 mAb (KPL1; BD Biosciences), which blocks EV71 binding to PSGL-1, as described previously (Nishimura *et al.*, 2009). Briefly, the cells in 48-well tissue culture plates (4×10^4 cells per well) were infected with viruses of 4×10^4 $CCID_{50}$ for 1 h at 34 °C. We inoculated the cells with KED005 of 4×10^3 $CCID_{50}$, as we could not obtain sufficient viral titre for KED005-LPS2. For mAb inhibition, we pretreated the cells with 10 μg ml^{-1} mAb [KPL1 or isotype control (MOPC-21; BioLegend)] for 1 h prior to infection, washed the cells, and maintained them in medium with 10 μg ml^{-1} mAb. At 4 days post-infection, the infected cells and supernatants were freeze–thawed, and viral titres were determined by calculating $CCID_{50}$ with a microtitration assay in RD cells as described previously (Nagata *et al.*, 2002). All infection assays were carried out in triplicate, and the mean viral titres were compared using Student's *t*-test. *P*-values <0.01 were considered statistically significant. As a PSGL-1-negative control, we used L-bsd cells (L929 cells transfected with an empty plasmid and selected in the presence of blasticidin) (Nishimura *et al.*, 2009).

The original 1095 strain replicated in L-PSGL-1 cells, but not in L-bsd cells (Fig. 1), which do not express human PSGL-1, as reported previously (Nishimura *et al.*, 2009). The viral titres of the original 1095 strain at 0 h and 4 days post-infection were reduced in the presence of anti-PSGL-1 mAb, but not in the presence of an isotype control (Fig. 1). These results confirmed that the original 1095 strain replicated in a PSGL-1-dependent manner, as reported previously (Nishimura *et al.*, 2009). The viral titres of the other original EV71 strains in L-PSGL-1 cells were significantly higher than titres in L-bsd cells 0 h post-infection, and the viral titres were reduced by anti-PSGL-1 mAb (Fig. 1). These results indicate that original EV71 bound to L-PSGL-1 cells in a PSGL-1-dependent manner. However, the viral titre of original EV71, except the 1095 strain, remained low in L-PSGL-1 cells even after 4 days (Fig. 1). On the other hand, all EV71-LPS variants replicated well in L-PSGL-1 cells, but not in L-bsd cells. The replication of EV71-LPS variants was inhibited by anti-PSGL-1 mAb, but not by the isotype control (Fig. 1). These results indicated that EV71-LPS variants replicated in L-PSGL-1 cells in a PSGL-1-dependent manner.

To compare viral replication kinetics of the original EV71 and L-PSGL-1-adapted variant in human cells, we infected

Table 1. PSGL-1-binding EV71 strains

Strain (sub-genogroup)	Major symptom	Specimen	Cell*	Location	Year	GenBank accession no.		Reference
						Original	LPS variant	
1095 (C2)	HFMD†	Throat swab	RD	Japan	1997	AB550332	AB550333	Nagata *et al.* (2002); Shimizu *et al.* (2004)
SK-EV006 (B3)	Encephalitis (fatal)	Rectal swab	Vero	Malaysia	1997	AB550334	AB550335	Shimizu *et al.* (1999)
C7/Osaka (B4)	Encephalitis (fatal)	Stool	Vero	Japan	1997	AB550336	AB550337	Shimizu *et al.* (1999)
75-Yamagata (C4)	HFMD†	Nasopharyngeal swab	RD	Japan	2003	AB550338	AB550339	Mizuta *et al.* (2005)
KED005 (C1)	HFMD†	Stool	RD	Malaysia	1997	AB550340	AB550341	Shimizu *et al.* (1999)

*The cell line used to prepare the original EV71 strains in this study.
†Hand, foot, and mouth disease.

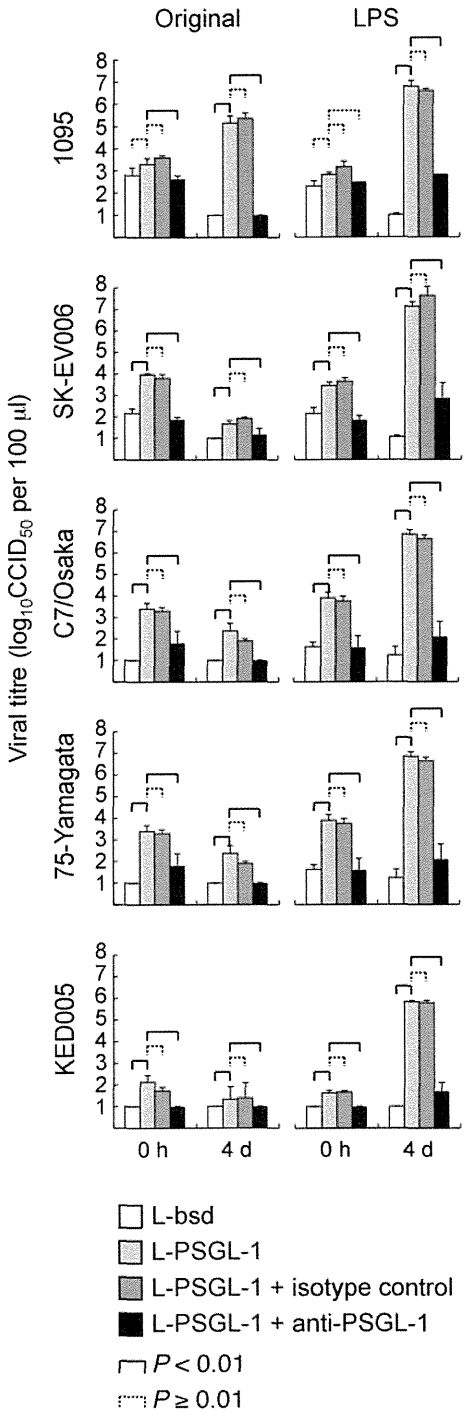

Fig. 1. EV71 replication in L-PSGL-1 cells in the presence of a PSGL-1-specific mAb. L-bsd cells were used as a PSGL-1-negative control.

PSGL-1-negative (RD), PSGL-1-positive (Jurkat) and human peripheral blood mononuclear cells (PBMC; purchased from Lonza Japan Ltd) with the original 1095 strain or 1095-LPS1 variant. RD (2.5×10^4 cells), Jurkat (4×10^4 cells) and human PBMC (2×10^5 cells) were inoculated with viruses of 2.5×10^4 (original 1095) or 2.5×10^3 (1095-LPS1) $CCID_{50}$ for 1 h at 37 °C (RD) or on ice (Jurkat or PBMC), washed and incubated in medium at 37 °C (RD) or 34 °C (Jurkat or PBMC). The original 1095 and 1095-LPS1 strains showed comparable replication kinetics in RD and Jurkat cells, and both of the EV71 strains did not grow well in human PBMC (Supplementary Fig. S2, available in JGV Online). We then tested the PSGL-1-dependent replication competence of other EV71-LPS variants in Jurkat cells, as described previously (Nishimura *et al.*, 2009). All five EV71-LPS variants replicated in Jurkat T cells in a PSGL-1-dependent manner, as demonstrated by the reduction of viral titres by anti-PSGL-1 mAb blockage at 3 days post-inoculation (Supplementary Fig. S3, available in JGV Online). These results indicate that the phenotypic difference between the original and L-PSGL-1-adapted EV71 strains was apparent in mouse L-PSGL-1 cells but not in human cells.

Finally, we examined mutations in the genomes of EV71 during the course of replication in L-PSGL-1 cells. We compared the complete nucleotide and deduced amino acid sequences between the original EV71 strains and the EV71-LPS variants. We extracted viral genomic RNA from the culture fluid of infected cells. We performed RT-PCR preparation of DNA fragments for DNA sequencing. The 5′ and 3′ ends of the viral genome were sequenced using the conventional RACE methods.

1095-LPS1 had two amino acid substitutions at VP2-K149M and VP3-Y29H compared with the original 1095 strain (Fig. 2). SK-EV006-LPS1 had four nucleotide mutations compared with the original SK-EV006 strain. Three out of the four mutations changed Y (C or T) to C or T in the 5′ non-translated region (NTR) and the region encoding non-structural proteins. The other mutation (A1398T) caused an amino acid substitution at VP2-K149I (Fig. 2). C7/Osaka-LPS1 and 75-Yamagata-LPS1 had only one amino acid substitution at VP2-K149 compared with the corresponding original EV71 strains (Fig. 2). Taken together, all four EV71-LPS1 variants had an amino acid substitution at VP2-K149I/M. Although the KED005-LPS2 variant did not have an amino acid substitution in VP2-K149, it had five amino acid substitutions in VP2 and VP1 (Fig. 2).

Previous studies have shown that the expression of specific cellular receptors for human enteroviruses on the cell surface of rodent cells allows effective viral replication similar to that in human susceptible cells expressing the corresponding viral receptors [human poliovirus receptor (Mendelsohn *et al.*, 1989), human intercellular adhesion molecule-1 (Shafren *et al.*, 1997), and human coxsackievirus and adenovirus receptor (Bergelson *et al.*, 1997)]. In the case of EV71, mouse L929 cells expressing human SCARB2 exhibit high susceptibility to EV71, which is comparable to human RD cells (Yamayoshi *et al.*, 2009). These results suggest that the efficacy of replication of enteroviruses, including EV71, mainly depends on the

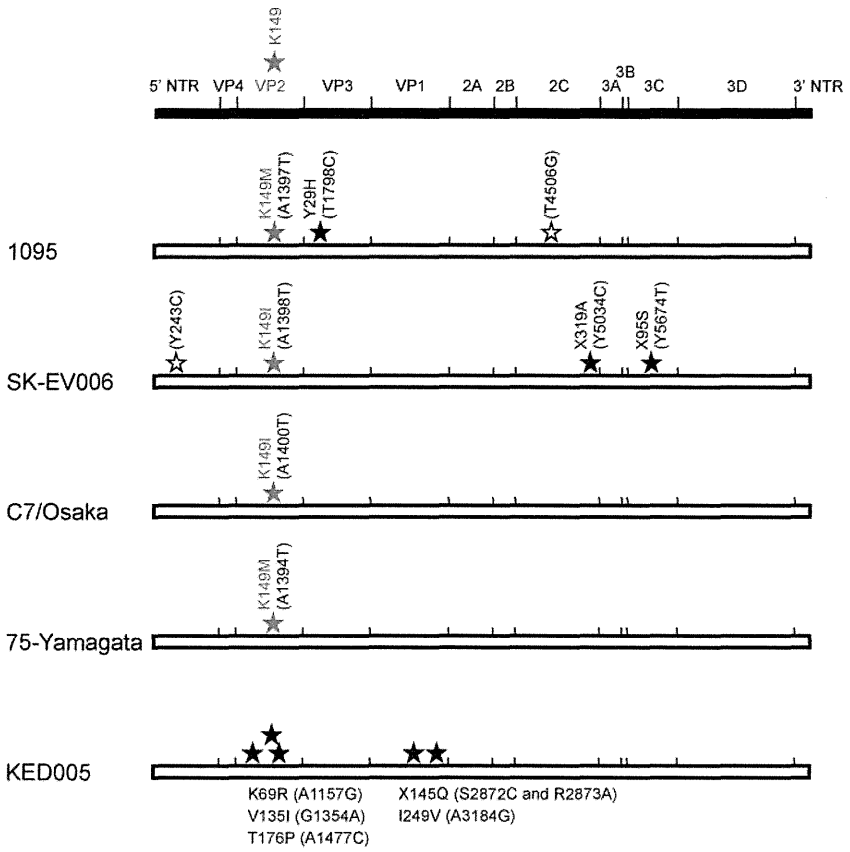

Fig. 2. Schematic of mutations identified in EV71-LPS1 (1095, SK-EV006, C7/Osaka and 75-Yamagata) and EV71-LPS2 (KED005) compared with the corresponding original EV71 strains. Amino acid substitutions observed in EV71-LPS are shown as black stars and VP2-149 are indicated as grey stars. A synonymous mutation and a mutation in the 5′ NTR are shown as white stars. The amino acid X indicates that its codon contains mixed nucleotides.

expression of specific receptors on the cell surface, even for rodent cell lines that are naturally non-permissive for enterovirus infection. In other words, after virus binding, entry and uncoating steps, which may be facilitated by virus-receptor interactions, rodent cells may support efficient viral replication of human enteroviruses.

On the other hand, not only the binding capability of the EV71 strains to PSGL-1, but also an adaptive mutation(s) in the capsid proteins was required for efficient viral replication of PSGL-1-binding strains of EV71 in L-PSGL-1 cells. A previous study using infectious molecular clones of EV71 revealed that a mutation at VP2-K149I is critical for efficient virus replication in Chinese hamster ovary cells (Chua *et al.*, 2008). In addition, one of the adaptive mutations was identified at VP2-K149 during the course of *in vivo* adaptation of EV71 by serial passaging of the virus in mouse brain (Wang *et al.*, 2004). Furthermore, a mouse-adapted EV71 variant (Nagoya-2876A strain) derived from a cDNA of the Nagoya strain of EV71 contains Ile at VP2-149 instead of the Lys residue that is conserved among other EV71 strains (Arita *et al.*, 2008). These results suggest that an amino acid substitution at VP2-K149 plays a critical role in the *in vitro* and *in vivo* adaptation of EV71 in rodent cells. Like human fibroblast cell lines, mouse L929 cells do not express detectable levels of mouse PSGL-1 (Thomas *et al.*, 2009). Therefore, mouse-adaptive mutations in the capsid proteins of EV71 may not be directly associated with a phenotypic change in EV71 variants with receptor-binding capability to mouse PSGL-1. For mouse-adapted poliovirus variants, some of the mouse adaptation determinants in the capsid proteins involve the efficacy of viral uncoating (Couderc *et al.*, 1996) and the others might be responsible for binding of the mutants to unidentified mouse receptor (Murray *et al.*, 1988). Likewise, it remains uncertain whether a mutation at VP2-K149 of EV71 is responsible for the change in tropism in a receptor-dependent or -independent manner.

Four out of five LPS variants, including 1095-LPS, contained an amino acid substitution at VP2-K149 after a single passage of the original EV71 strains in L-PSGL-1 cells. The VP2-K149 substitution confers only one amino acid difference between the original EV71 strains and the LPS variants of the C7/Osaka and 75-Yamagata strains, suggesting that the single amino acid at VP2-149 is a potential determinant for the adaptation phenotype of EV71 to L-PSGL-1 cells. For the KED005-LPS2 variant, an amino acid change at VP2-K149 was not identified, but instead, multiple amino acid substitutions (three in VP2 and two in VP1) were found after a second passage in L-PSGL-1 cells. Further analysis using infectious clones of EV71 will be required to elucidate the contribution of possible determinants for adaptation to mouse cells.

Mouse L929 cell lines expressing the human poliovirus receptor have played a critical role in laboratory diagnosis of polioviruses for global polio eradication (Hovi &

Stenvik, 1994; Pipkin *et al.*, 1993). Mouse cell lines expressing specific cellular receptors for EV71, PSGL-1 and SCARB2, may also be useful for receptor-specific isolation and identification of EV71 from clinical samples (Nishimura *et al.*, 2009; Yamayoshi *et al.*, 2009). However, as we have shown in this study, along with the PSGL-1-binding phenotype of EV71, the adaptation and selection bias among EV71 variants to grow in L-PSGL-1 cells should be carefully considered. Likewise, the mouse-adaptive phenotype of the EV71 strains and variants should also be taken into account when establishing transgenic mouse models carrying human receptors for EV71.

Acknowledgements

We are grateful to Junko Wada for excellent technical assistance. This work was supported by a Grant-in-Aid for Young Scientists (B, 21790452) from the Ministry of Education, Culture, Sports, Science and Technology, Japan (Y. N.). Y. N. and H. S. were supported in part by a Grant-in-Aid for Research on Emerging and Re-emerging Infectious Diseases and a Grant-in-Aid for the Promotion of Polio Eradication from the Ministry of Health, Labour and Welfare, Japan.

References

Arita, M., Ami, Y., Wakita, T. & Shimizu, H. (2008). Cooperative effect of the attenuation determinants derived from poliovirus Sabin 1 strain is essential for attenuation of enterovirus 71 in the NOD/SCID mouse infection model. *J Virol* **82**, 1787–1797.

Bergelson, J. M., Cunningham, J. A., Droguett, G., Kurt-Jones, E. A., Krithivas, A., Hong, J. S., Horwitz, M. S., Crowell, R. L. & Finberg, R. W. (1997). Isolation of a common receptor for coxsackie B viruses and adenoviruses 2 and 5. *Science* **275**, 1320–1323.

Chan, L. G., Parashar, U. D., Lye, M. S., Ong, F. G. L., Zaki, S. R., Alexander, J. P., Ho, K. K., Han, L. L., Pallansch, M. A. & other authors (2000). Deaths of children during an outbreak of hand, foot, and mouth disease in Sarawak, Malaysia: clinical and pathological characteristics of the disease. *Clin Infect Dis* **31**, 678–683.

Chua, B. H., Phuektes, P., Sanders, S. A., Nicholls, P. K. & McMinn, P. C. (2008). The molecular basis of mouse adaptation by human enterovirus 71. *J Gen Virol* **89**, 1622–1632.

Couderc, T., Delpeyroux, F., Le Blay, H. & Blondel, B. (1996). Mouse adaptation determinants of poliovirus type 1 enhance viral uncoating. *J Virol* **70**, 305–312.

Eskelinen, E. L., Tanaka, Y. & Saftig, P. (2003). At the acidic edge: emerging functions for lysosomal membrane proteins. *Trends Cell Biol* **13**, 137–145.

Ho, M., Chen, E. R., Hsu, K. H., Twu, S. J., Chen, K. T., Tsai, S. F., Wang, J. R. & Shih, S. R. (1999). An epidemic of enterovirus 71 infection in Taiwan. *N Engl J Med* **341**, 929–935.

Hovi, T. & Stenvik, M. (1994). Selective isolation of poliovirus in recombinant murine cell line expressing the human poliovirus receptor gene. *J Clin Microbiol* **32**, 1366–1368.

Laszik, Z., Jansen, P. J., Cummings, R. D., Tedder, T. F., McEver, R. P. & Moore, K. L. (1996). P-selectin glycoprotein ligand-1 is broadly expressed in cells of myeloid, lymphoid, and dendritic lineage and in some nonhematopoietic cells. *Blood* **88**, 3010–3021.

McMinn, P. C. (2002). An overview of the evolution of enterovirus 71 and its clinical and public health significance. *FEMS Microbiol Rev* **26**, 91–107.

Mendelsohn, C. L., Wimmer, E. & Racaniello, V. R. (1989). Cellular receptor for poliovirus: molecular cloning, nucleotide sequence, and expression of a new member of the immunoglobulin superfamily. *Cell* **56**, 855–865.

Mizuta, K., Abiko, C., Murata, T., Matsuzaki, Y., Itagaki, T., Sanjoh, K., Sakamoto, M., Hongo, S., Murayama, S. & Hayasaka, K. (2005). Frequent importation of enterovirus 71 from surrounding countries into the local community of Yamagata, Japan, between 1998 and 2003. *J Clin Microbiol* **43**, 6171–6175.

Murray, M. G., Bradley, J., Yang, X. F., Wimmer, E., Moss, E. G. & Racaniello, V. R. (1988). Poliovirus host range is determined by a short amino acid sequence in neutralization antigenic site I. *Science* **241**, 213–215.

Nagata, N., Shimizu, H., Ami, Y., Tano, Y., Harashima, A., Suzaki, Y., Sato, Y., Miyamura, T., Sata, T. & Iwasaki, T. (2002). Pyramidal and extrapyramidal involvement in experimental infection of cynomolgus monkeys with enterovirus 71. *J Med Virol* **67**, 207–216.

Nishimura, Y., Shimojima, M., Tano, Y., Miyamura, T., Wakita, T. & Shimizu, H. (2009). Human P-selectin glycoprotein ligand-1 is a functional receptor for enterovirus 71. *Nat Med* **15**, 794–797.

Pipkin, P. A., Wood, D. J., Racaniello, V. R. & Minor, P. D. (1993). Characterisation of L cells expressing the human poliovirus receptor for the specific detection of polioviruses *in vitro*. *J Virol Methods* **41**, 333–340.

Sako, D., Chang, X. J., Barone, K. M., Vachino, G., White, H. M., Shaw, G., Veldman, G. M., Bean, K. M., Ahern, T. J. & other authors (1993). Expression cloning of a functional glycoprotein ligand for P-selectin. *Cell* **75**, 1179–1186.

Shafren, D. R., Dorahy, D. J., Greive, S. J., Burns, G. F. & Barry, R. D. (1997). Mouse cells expressing human intercellular adhesion molecule-1 are susceptible to infection by coxsackievirus A21. *J Virol* **71**, 785–789.

Shimizu, H., Utama, A., Yoshii, K., Yoshida, H., Yoneyama, T., Sinniah, M., Yusof, M. A. B., Okuno, Y., Okabe, N. & other authors (1999). Enterovirus 71 from fatal and nonfatal cases of hand, foot and mouth disease epidemics in Malaysia, Japan and Taiwan in 1997–1998. *Jpn J Infect Dis* **52**, 12–15.

Shimizu, H., Utama, A., Onnimala, N., Li, C., Li-Bi, Z., Yu-Jie, M., Pongsuwanna, Y. & Miyamura, T. (2004). Molecular epidemiology of enterovirus 71 infection in the Western Pacific Region. *Pediatr Int* **46**, 231–235.

Thomas, G. M., Panicot-Dubois, L., Lacroix, R., Dignat-George, F., Lombardo, D. & Dubois, C. (2009). Cancer cell-derived microparticles bearing P-selectin glycoprotein ligand 1 accelerate thrombus formation *in vivo*. *J Exp Med* **206**, 1913–1927.

Wang, Y. F., Chou, C. T., Lei, H. Y., Liu, C. C., Wang, S. M., Yan, J. J., Su, I. J., Wang, J. R., Yeh, T. M. & other authors (2004). A mouse-adapted enterovirus 71 strain causes neurological disease in mice after oral infection. *J Virol* **78**, 7916–7924.

Yamayoshi, S., Yamashita, Y., Li, J., Hanagata, N., Minowa, T., Takemura, T. & Koike, S. (2009). Scavenger receptor B2 is a cellular receptor for enterovirus 71. *Nat Med* **15**, 798–801.

Yang, F., Ren, L., Xiong, Z., Li, J., Xiao, Y., Zhao, R., He, Y., Bu, G., Zhou, S. & other authors (2009). Enterovirus 71 outbreak in the People's Republic of China in 2008. *J Clin Microbiol* **47**, 2351–2352.

JOURNAL OF VIROLOGY, May 2011, p. 4937–4946 Vol. 85, No. 10
0022-538X/11/$12.00 doi:10.1128/JVI.02358-10

Identification of a Human SCARB2 Region That Is Important for Enterovirus 71 Binding and Infection[▽]

Seiya Yamayoshi and Satoshi Koike*

Neurovirology Project, Tokyo Metropolitan Institute of Medical Science, Tokyo Metropolitan Organization for Medical Research, 2-1-6, Kamikitazawa, Setagaya-ku, Tokyo 156-8506, Japan

Received 10 November 2010/Accepted 28 February 2011

We previously identified human scavenger receptor class B, member 2 (SCARB2), as a cellular receptor for enterovirus 71 (EV71). Expression of human SCARB2 (hSCARB2) permitted mouse L929 cells to efficiently bind to virions and to produce both viral proteins and progeny viruses upon EV71 infection. Mouse Scarb2 (mScarb2) exhibited 85.8% amino acid identity and 99.9% similarity to hSCARB2. The expression of mScarb2 in L929 cells conferred partial susceptibility. Very few virions bound to mScarb2-expressing cells. The viral titer in L929 cells expressing mScarb2 was approximately 40- to 100-fold lower than that in L929 cells expressing hSCARB2. Using hSCARB2–mScarb2 chimeric mutants, we attempted to map the region that was important for efficient EV71 infection. L929 cells expressing chimeras that carried amino acids 142 to 204 from the human sequence were susceptible to EV71, while chimeras that carried the mouse sequence in this region were not. Moreover, this region was also critical for binding to virions. The determination of this region in hSCARB2 that is important for EV71 binding and infection greatly contributes to the understanding of virus-receptor interactions. Further studies will clarify the early steps of EV71 infection.

Enterovirus 71 (EV71), together with coxsackievirus A16 (CVA16), belongs to human enterovirus species A of the genus *Enterovirus* within the family *Picornaviridae* (28). The virus contains a single-stranded, positive-sense RNA surrounded by an icosahedral capsid assembled from 60 copies of each of the four structural proteins: VP1, VP2, VP3, and VP4 (32). EV71 was first isolated from patients with neurological diseases, including fatal encephalitis and aseptic meningitis, in California from 1969 to 1972 (33). Later studies revealed that EV71 is associated with hand-foot-and-mouth disease (HFMD) in young children and infants (6, 13). Although HFMD is generally considered a mildly infectious disease, HFMD caused by EV71, but not by other enteroviruses, is sometimes involved with severe neurological diseases, including brain stem encephalitis and acute flaccid paralysis (23). In recent years, epidemic or sporadic outbreaks of neurovirulent EV71 infections have been reported mainly in Southeast or East Asia, including Taiwan, Malaysia, Singapore, Japan, and China (1, 8, 11, 17, 27, 38). In particular, the epidemic outbreaks that occurred in 2008 and 2009 in China resulted in a total of 488,955 and 1,155,525 HFMD cases, including 126 and 353 fatal cases per year, respectively (http://www.moh.gov.cn/publicfiles/business/htmlfiles/mohbgt/s3582/201002/46043.htm) (40). Moreover, the EV71 epidemic has since continued in China, with 987,779 HFMD cases, including 537 fatal cases reported as of 22 June 2010 (http://www.moh.gov.cn/publicfiles/business/htmlfiles/mohbgt/s3582/201006/47871.htm).

Human RD cells are highly susceptible to EV71 infection, whereas mouse L929 cells exhibit very low susceptibility. We previously reported the identification of EV71 receptors by genetic complementation of L929 cells with genes transferred from human RD cells (37). Briefly, we established two EV71-susceptible cell lines that carried a portion of human genomic DNA. By identifying the integrated human DNA in one of the transformants, Ltr051 cells, we have shown that scavenger receptor class B, member 2 (SCARB2), is a cellular receptor for EV71. SCARB2 serves as a receptor for all EV71 isolates tested. EV71 infection in the SCARB2-expressing L929 cell line is as efficient as that in the RD cell line (37). We have also found that virus replication efficiency in another transformant cell line, Ltr246, is slightly lower than that in Ltr051 cells (37) and that Ltr246 cells are susceptible to only a subset of EV71 strains (S. Yamayoshi et al., unpublished data). Although Ltr246 cells appear to express another, unknown receptor (receptor X), we have not yet identified the human DNA sequence that confers susceptibility on Ltr246 cells. In addition, Nishimura et al. also have identified the selectin P ligand (SELPLG, also known as P-selectin glycoprotein ligand-1 [PSGL-1]) as an EV71 receptor from human T cell leukemia Jurkat cells by using the panning assay, which enriched for molecules with strong binding affinity to EV71 particles (26). SELPLG also confers susceptibility only to some EV71 strains on L929 cells. In Jurkat cells and L929 cells expressing SELPLG, however, the appearance of cytopathic effect (CPE) and the expression of viral proteins after EV71 infection occurred more slowly than in RD cells and L929 cells expressing SCARB2 (26). We have confirmed that Ltr246 cells do not carry the human *SCARB2* and *SELPLG* genes. Another study has shown that the depletion of O-linked glycans or pretreatment with sialidase reduced EV71 infection in DLD-1 human colon cancer cells (39). These results suggest that EV71 can enter the cell via multiple pathways. Because all EV71 strains tested used SCARB2 as the receptor (37), whereas only a subset of EV71 strains used SELPLG (26) or receptor X,

* Corresponding author. Mailing address: Neurovirology Project, Tokyo Metropolitan Institute of Medical Science, Tokyo Metropolitan Organization for Medical Research, 2-1-6, Kamikitazawa, Setagaya-ku, Tokyo 156-8506, Japan. Phone: 81-3-5316-3312. Fax: 81-3-5316-3224. E-mail: koike-st@igakuken.or.jp.

▽ Published ahead of print on 9 March 2011.

SCARB2 may play a central role in the early steps of EV71 infection. Therefore, characterizations of the role of SCARB2 during EV71 infection will contribute to the understanding of EV71 entry.

SCARB2 (also known as lysosomal integral membrane protein II, or CD36b like-2) belongs to the CD36 family and has two transmembrane domains, with the N and C termini located in the cytosol (10). SCARB2 is one of the most abundant proteins in the lysosomal membrane and participates in membrane transport and the reorganization of the endosomal/lysosomal compartment (21). SCARB2 also works as the receptor for the mannose-6-phosphate-independent transport of β-glucocerebrosidase (β-GC) to the lysosome (5, 30). The binding of β-GC to SCARB2 occurs within the luminal domain of SCARB2, particularly in the coiled-coil motif at amino acids 152 to 167 (30). SCARB2 deficiency in mice causes ureteropelvic junction obstruction, deafness, and peripheral neuropathy (12). Although the motifs in some cellular receptors for picornaviruses that are important for binding and/or infection have been elucidated, SCARB2 has no motifs common to other picornavirus receptors, such as an immunoglobulin (Ig)-like motif. Thus, SCARB2 is a new class of picornavirus receptor. The identification of important regions in SCARB2 would contribute to the elucidation of the virus-receptor interaction.

In this report, we compared the susceptibilities of cells expressing human SCARB2 (hSCARB2) or mouse Scarb2 (mScarb2) to EV71. Additionally, we mapped the region in hSCARB2 that is important for EV71 infection by using hSCARB2–mScarb2 chimeras.

MATERIALS AND METHODS

Cells. Human RD cells, mouse L929 cells, and African green monkey Vero cells were cultured in Dulbecco's modified Eagle medium (DMEM; Sigma) supplemented with 5% fetal bovine serum (FBS) and a penicillin-streptomycin solution (Invitrogen) (5% FBS-DMEM).

Viruses. EV71 strain SK-EV006/Malaysia/97 was propagated in Vero cells for use in this study (25). EV71-GFP, which expresses green fluorescent protein (GFP) upon viral replication, was recovered from an infectious cDNA clone, pSVA-EV71-GFP, which has been described previously (37).

Plasmids. The cDNA fragment of mScarb2 was amplified by reverse transcription-PCR (RT-PCR) from L929 cells with primers mSCARB2-Eco(+) (CAGA ATTCACCATGGGCAGATGCTGCTTCTACA) and mSCARB2-Xba(−) (CA CATCTAGATTAGGTTCGTATGAGGGGTGCT), and the PCR product was inserted into pCAGGS-PUR (14). The resulting construct was designated pCA-mScarb2. A cDNA fragment encoding mScarb2 or hSCARB2 (37) was subcloned into pCAGGS.MCS (19, 36) to create a FLAG tag at the C terminus, and the construct was designated pCA-mScarb2-F or pCA-hSCARB2-F, respectively.

Chimeric hSCARB2–mScarb2 mutants (see Fig. 6A and 7A) were constructed using standard PCR-based methods and were cloned into pCAGGS.MCS with a FLAG tag at the C terminus. The mutants did not have unexpected mutations or deletions.

Viral spread in cell culture. RD cells were infected with either EV71-GFP or EV71. At 24 h postinfection, cells infected with EV71-GFP were imaged with IX70 and DP70 cameras (Olympus) and were analyzed using DP Controller software (Olympus). The cells infected with EV71 or EV71-GFP were subsequently fixed with 4% paraformaldehyde and were probed with a mouse anti-EV71 antibody (clone 422-8D-4C-4D; Millipore), followed by incubation with an Alexa Fluor 488 donkey anti-mouse IgG (Invitrogen). Images were acquired using the IX70 camera.

PNGase F digestion. L929 cells were transfected with the plasmid encoding hSCARB2, mScarb2, hSCARB2-F, mScarb2-F, H(M4)-F, M(H2)-F, or M(H3)-F using the FuGENE 6 transfection reagent. After 48 h, the transfected cells were lysed with glycoprotein denaturing buffer (New England Biolabs [NEB]) and were then incubated for 10 min at 99°C. Denatured samples were mixed with G7 reaction buffer (NEB) supplemented with 1% NP-40 and 500 U peptide *N*-glycosidase F (PNGase F) (NEB) and were then incubated for 2 h at 37°C for digestion. These samples were mixed with a sodium dodecyl sulfate (SDS) sample buffer and were then incubated for 5 min at 95°C before being resolved on a 12% Tris-glycine gel. Resolved proteins were probed with a goat anti-hSCARB2 antibody (R&D Systems), a goat anti-mScarb2 antibody (R&D Systems), or a rabbit anti-FLAG antibody (Sigma), followed by incubation with a horseradish peroxidase (HRP)-conjugated anti-goat or anti-rabbit antibody (Jackson ImmunoResearch).

Single-round infection assay. L929 cells were transfected with the indicated plasmid in triplicate to analyze (i) transfection efficiency, (ii) protein expression, and (iii) EV71-GFP infection. Transfected cells in the first well were fixed at the plate bottom with 4% paraformaldehyde at 48 h posttransfection and were probed with the mouse anti-FLAG antibody (Sigma), followed by incubation with Alexa Fluor 488 donkey anti-mouse IgG. Images were acquired using the IX70 and DP70 cameras. Transfected cells in the second well were mixed with SDS sample buffer (Invitrogen) at 48 h posttransfection, and these samples were incubated for 5 min at 95°C before being resolved on a 12% Tris-glycine gel (Invitrogen). Resolved proteins were probed with the anti-hSCARB2 antibody, the rabbit anti-FLAG antibody (Sigma), or a mouse antibody against β-actin (ACTB) (clone AC-74; Sigma), followed by incubation with the appropriate HRP-conjugated secondary antibody (Jackson ImmunoResearch). Transfected cells in the third well were infected with EV71-GFP at 24 h after transfection and were incubated for another 24 h at 37°C. Subsequently, images were acquired using the IX70 and DP70 cameras and were analyzed using DP Controller software. Infected cells, including GFP-positive cells, were detached in trypsin-EDTA (0.05% trypsin, 0.53 mM EDTA · 4Na) (GIBCO) and were incubated with 4% paraformaldehyde for 30 min at room temperature. After being washed with phosphate-buffered saline (PBS) containing 2% FBS, the cells were analyzed with a FACSCalibur flow cytometer and CellQuest Pro software (both from Becton Dickinson and Company).

Multistep infection assay. L929 cells were transfected with the indicated plasmid using the FuGENE 6 transfection reagent. After 24 h, the transfected cells were infected with EV71 (1×10^3 50% tissue culture infective doses [$TCID_{50}$]) and were incubated for 0, 12, 24, 36, or 48 h at 37°C. At each time point, viral titers were determined and expressed as the $TCID_{50}$ according to the Reed-Muench method (31).

Immunoprecipitation assay. Pulldown assays were performed as reported previously (37) with some modifications. EV71 (1.87×10^8 $TICD_{50}$) was incubated with bovine serum albumin (BSA) (10 μg), human IgG Fc (control Fc) (10 μg; R&D Systems), hSCARB2-Fc (1, 3, or 10 μg; R&D Systems), or mScarb2-Fc (1, 3, or 10 μg; R&D Systems) and anti-human IgG (Fc specific)-agarose (Sigma) in 1 ml of 5% FBS DMEM for 2 h at 4°C. The beads were then washed twice with 5% FBS-DMEM, suspended in SDS sample buffer, and incubated for 10 min at 95°C. After the beads were removed, the samples were loaded onto a 12% Tris-glycine gel, followed by Western blotting with a rabbit anti-EV71 antibody (25) or an anti-human IgG Fc_γ fragment-specific antibody (Jackson ImmunoResearch). For deglycosylation, control Fc (3 μg) and hSCARB2-Fc (3 μg) in the native form were treated with 1,500 U PNGase F in G7 reaction buffer and were incubated for 24 h at 37°C before being mixed with anti-human IgG (Fc specific)-agarose.

Virus attachment assay. L929 cells transfected with the indicated plasmid were detached in PBS containing 0.05% EDTA. These cells were mixed with EV71 (1.87×10^8 $TICD_{50}$) for 1 h at 4°C, washed twice with 5% FBS-DMEM, suspended in SDS sample buffer, and then incubated for 10 min at 95°C. The samples were resolved by SDS-polyacrylamide gel electrophoresis (PAGE) using the 12% Tris-glycine gel, followed by Western blot analysis with an anti-EV71, anti-FLAG, or anti-ACTB antibody.

Biotinylation of cell surface proteins. L929 cells transfected with the indicated plasmids were washed twice with ice-cold PBS and were biotinylated twice with Sulfo-*N*-hydroxysuccinimide (NHS)-SS-Biotin (Pierce) for 15 min each time at 4°C. After two washes with ice-cold PBS, free thiol groups were quenched with quenching solution (Pierce), and the cells were solubilized in lysis buffer (20 mM Tris-HCl [pH 7.5], 150 mM NaCl, 1 mM EDTA, 1% Triton X-100, and Complete Mini protease inhibitor cocktail [Roche]) and were precipitated with NeutrAvidin agarose resin (Pierce). Precipitated proteins and cell lysates were analyzed by Western blotting with the anti-FLAG antibody.

RESULTS

Comparison of amino acid sequences of hSCARB2 and mScarb2. The cDNA encoding mScarb2 was prepared from

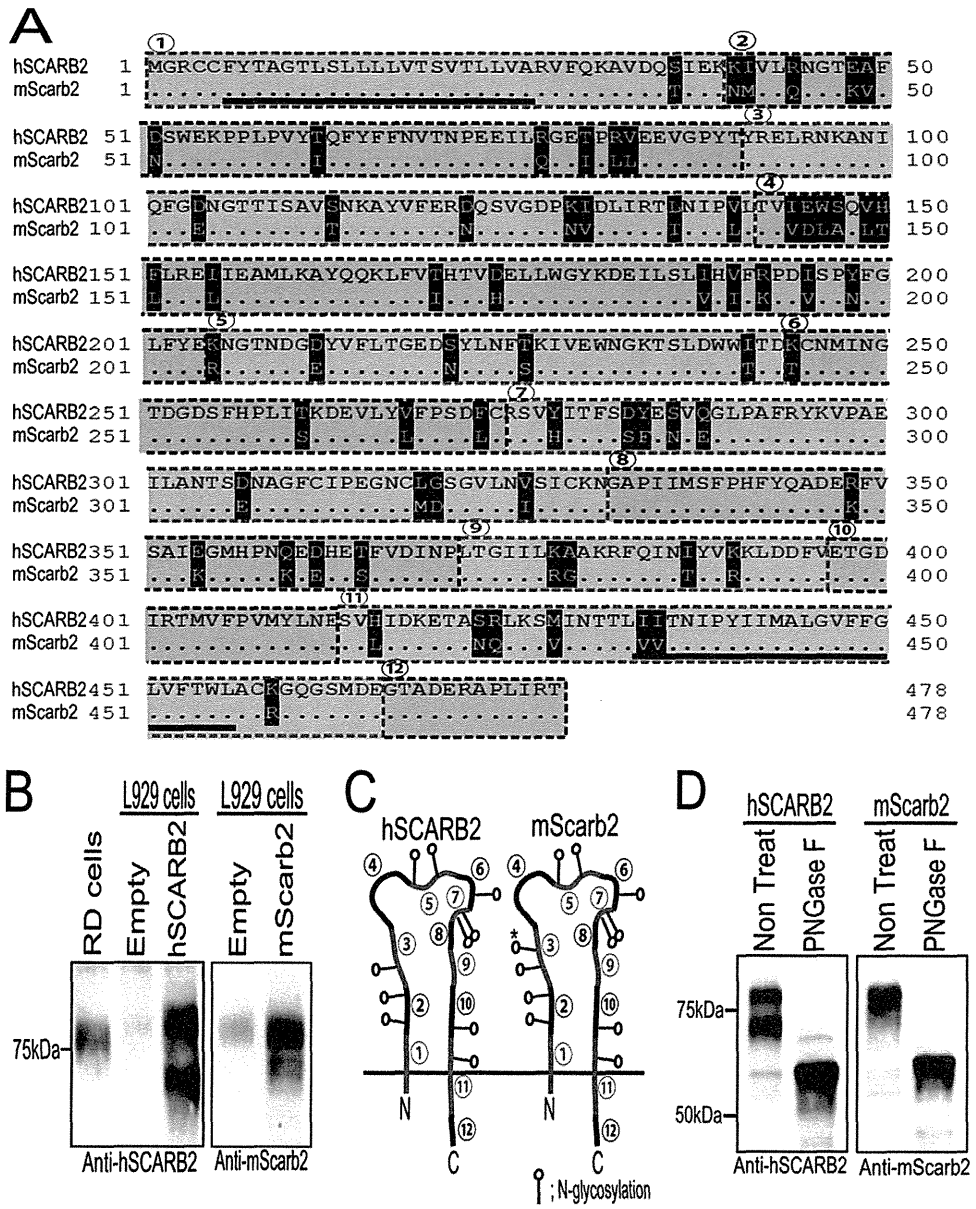

FIG. 1. Human SCARB2 and mouse Scarb2. (A) Comparison of the amino acid sequence of hSCARB2 with that of mScarb2. Divergent amino acids are highlighted. Two transmembrane domains are underlined, and the amino acids encoded in the mRNA from *SCARB2* exons 1, 3, 5, 7, 9, and 11 are outlined with red dashed lines. The amino acids encoded in the mRNA from exons 2, 4, 6, 8, 10, and 12 are outlined with black dashed lines. (B) Expression of hSCARB2 and mScarb2. L929 cells were transfected with plasmids encoding hSCARB2 or mScarb2. Transfected cells and RD cells were analyzed by Western blotting with an anti-hSCARB2 or anti-mScarb2 antibody. (C) Schematic diagrams of hSCARB2 and mScarb2. Red lines represent the amino acid sequences encoded in exons 1, 3, 5, 7, 9, and 11, and black lines represent those encoded in exons 2, 4, 6, 8, 10, and 12 (numbering from the N terminus to the C terminus). Potential N-glycosylation sites are indicated by lollipops. An asterisk marks the N-glycosylation site that is present only in mScarb2. (D) PNGase F treatment of hSCARB2 and mScarb2. L929 cells were transfected with plasmids encoding hSCARB2 or mScarb2. The cells were either left untreated (Non Treat) or treated with PNGase F, and the samples were analyzed by Western blotting with an anti-hSCARB2 or an anti-mScarb2 antibody.

L929 cells, and its amino acid sequence was compared with that of hSCARB2 (Fig. 1A). Both hSCARB2 and mScarb2 are composed of 478 amino acids, which are encoded in 12 exons. The level of amino acid identity between hSCARB2 and mScarb2 was 85.8%, and the level of similarity was 99.9%. We transiently expressed hSCARB2 and mScarb2 in L929 cells and detected the expressed proteins using anti-human and anti-mouse SCARB2 antibodies. We detected a single band that migrated at approximately 80 kDa in the Western blot of RD cells with anti-hSCARB2 antibody. mSCARB2, which is endogenously expressed in L929 cells, was detected in empty-vector-transfected L929 cells with an anti-mScarb2 antibody (Fig. 1B). We detected two major molecular species migrating at approximately 70 kDa and 80 kDa with an anti-hSCARB2 antibody in cells transfected with pCA-hSCARB2 (Fig. 1B, left). Similarly, we also detected two major molecular species

migrating at approximately 70 kDa and 80 kDa with an anti-mScarb2 antibody in cells transfected with pCA-mScarb2 (Fig. 1B, right). The apparent molecular sizes of these bands were larger than that deduced from the amino acid sequence (approximately 54 kDa). hSCARB2 and mScarb2 are reported to be N-glycosylated proteins in human and mouse cells, respectively (5, 30). hSCARB2 was found to have 10 potential N-glycosylation sites, whereas mScarb2 was found to have 11 (Fig. 1C). Potential N-glycosylation sites were found in the amino acid sequences encoded in exons 2, 3, 5, 6, 7, 10, and 11 of both hSCARB2 and mScarb2. mScarb2 had one additional potential N-glycosylation site in exon 3. To confirm whether exogenously expressed SCARB2s were glycosylated in L929 cells, cell lysates were treated with PNGase F, which removes all N-linked carbohydrate residues. After PNGase F treatment, hSCARB2 and mScarb2 were each detected as a single band at the calculated molecular mass (approximately 54 kDa) (Fig. 1D). These results indicate that hSCARB2 and mScarb2 are expressed as N-glycosylated proteins in mouse L929 cells and that the glycosylation pattern differs slightly from that of the endogenous proteins.

Strategy for the comparison of infection efficiencies in L929 cells expressing hSCARB2 or mScarb2. To compare the efficiency of a single round of EV71 infection via hSCARB2 versus mScarb2, we used EV71-GFP as a challenge virus. EV71-GFP, when used to infect cells, expresses sufficient levels of GFP to monitor the establishment of infection. This virus, however, had a defect in growth kinetics and in spreading. It was impossible to determine the viral titer either by plaque formation or by the $TCID_{50}$ method. When RD cells were infected with EV71-GFP at an appropriate dilution, GFP-positive cells became visible at approximately 16 to 18 h postinfection, suggesting that the kinetics of viral protein expression was unusual compared with that of wild-type virus. Clusters of GFP-positive or viral antigen-positive cells, which had spread from the initial infectious center, were not observed at 24 h postinfection (Fig. 2A, left and center). In contrast, when RD cells were infected with wild-type EV71, we observed clusters of viral antigen-positive cells that had formed due to spreading from the infectious centers at 24 h postinfection (Fig. 2A, right panel). Therefore, we evaluated the efficiency of EV71 infection at the initial round of infection by using EV71-GFP and counting the number of GFP-positive cells at 24 h postinfection.

To monitor the expression levels of hSCARB2 and mScarb2 by Western blotting, we added a FLAG epitope tag to the C termini of the proteins (5). To examine whether the C-terminal FLAG tag affected EV71 infection, we compared the numbers of GFP-positive cells after infection with EV71-GFP in L929 cells expressing hSCARB2 with or without the FLAG tag (Fig. 2B to E). L929 cells were transfected with pCA-hSCARB2 or pCA-hSCARB2-F, and after 24 h, the transfection efficiencies and expression of hSCARB2 and hSCARB2-F were confirmed by immune staining and Western blot analysis, respectively (Fig. 2B and C). The numbers of SCARB2-positive cells in L929 cells transfected with pCA-hSCARB2 or pCA-hSCARB2-F were comparable (Fig. 2B). Two major species of hSCARB2 and hSCARB2-F with similar intensities were detected by Western blotting using the anti-hSCARB2 antibody (Fig. 2C). Thus, the transfection efficiency, expression level,

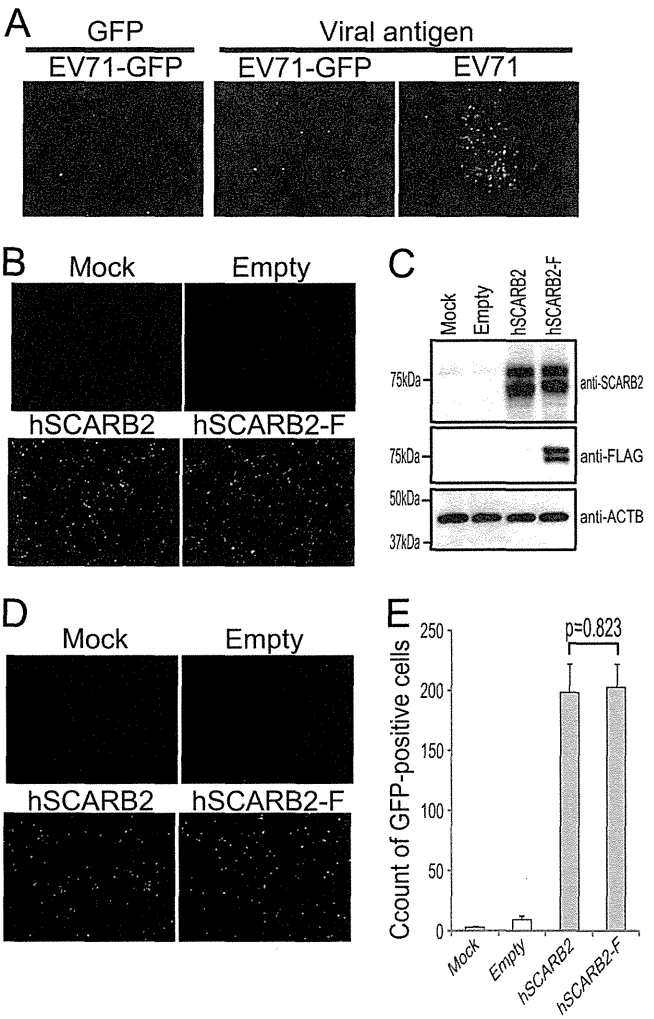

FIG. 2. Strategy for comparing infection efficiencies in L929 cells expressing hSCARB2 or mScarb2. (A) EV71-GFP is defective in viral spread. RD cells were infected with EV71 or EV71-GFP. Infected cells were imaged at 24 h postinfection in order to observe GFP via fluorescence microscopy (GFP) and were then stained with an anti-EV71 antibody. (B to E) Efficiency of EV71-GFP infection via hSCARB2 with or without the FLAG tag. (B) Transfection efficiency was assessed by immunostaining with an anti-hSCARB2 antibody. (C) Expression of hSCARB2 or hSCARB2-F was confirmed by Western blot analysis with an anti-hSCARB2 or an anti-FLAG antibody. Expression of β-actin (ACTB) was used as a loading control. (D and E) Cells infected with EV71-GFP were imaged via fluorescence microscopy (D) and were concomitantly analyzed by FACS to quantify the number of GFP-positive cells (E). The FACS data are shown as mean counts with standard deviations ($n = 3$). Statistical significance was determined by Student's t test. There was no significant difference between hSCARB2 and hSCARB2-F ($P = 0.823$).

and glycosylation pattern of hSCARB2 were not affected by the addition of the FLAG tag. Under these conditions, these transfected L929 cells were infected with EV71-GFP and were imaged at 24 h postinfection (Fig. 2D). No GFP-positive cells were observed in the mock-transfected or empty-plasmid-transfected cells, whereas many GFP-positive cells were detected in the hSCARB2- and hSCARB2-F-transfected cells (Fig. 2D). To quantify the microscopic observations, these cells were analyzed by fluorescence-activated cell sorting (FACS) to

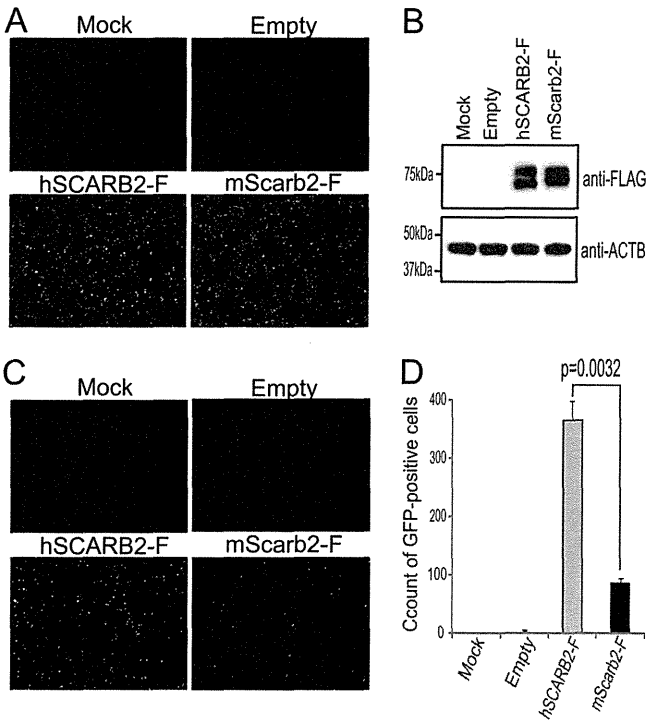

FIG. 3. Efficiencies of EV71-GFP infection via hSCARB2 or mScarb2. Single-round infection assays were performed to compare the efficiencies of EV71 infection via hSCARB2-F versus mScarb2-F. (A and B) The transfection efficiencies and expression of hSCARB2-F and mScarb2-F were confirmed by immunostaining (A) and Western blot analysis with an anti-FLAG antibody (B), respectively. ACTB was used as a loading control for the Western blot. (C and D) The transfected cells infected with EV71-GFP were imaged via fluorescence microscopy (C) and were then analyzed by FACS (D). The FACS data are shown as mean counts with standard deviations (n = 3). Statistical significance was determined by Student's t test.

count the number of GFP-positive cells (Fig. 2E). As reported previously, the number of GFP-positive cells was significantly greater in cells expressing hSCARB2 or hSCARB2-F than in mock- or empty plasmid-transfected cells ($P < 0.01$) (37). There was no significant difference in the number of GFP-positive cells between hSCARB2- and hSCARB2-F-expressing cells ($P = 0.823$). Similar results were obtained using nontagged and FLAG-tagged mScarb2 (data not shown). These results clearly show that EV71 infection via SCARB2 was not affected by the C-terminal FLAG tag. From these results, we could compare the efficiencies of EV71-GFP infection using this assay.

EV71-GFP infection of L929 cells expressing hSCARB2 and mScarb2. We conducted the single-round infection assay to compare the efficiencies of EV71 infection in L929 cells expressing hSCARB2-F versus mScarb2-F (Fig. 3). L929 cells were either mock transfected or transfected with pCA-hSCARB2-F, pCA-mScarb2-F, or an empty plasmid. After confirmation of transfection efficiency and expression of hSCARB2-F and mScarb2-F by immune staining and Western blotting (Fig. 3A and B), the transfected cells were infected with EV71-GFP and were observed at 24 h postinfection (Fig. 3C). No GFP-positive cells were found in mock- or empty-plasmid-transfected cells. A large number of GFP-positive

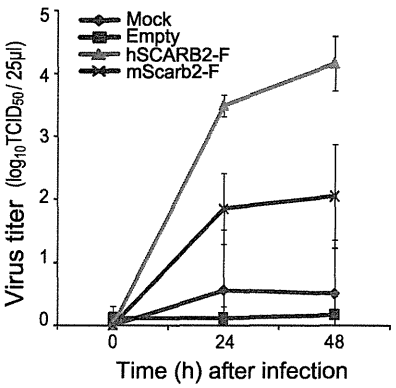

FIG. 4. Multistep infections of EV71 in L929 cells expressing hSCARB2 or mScarb2. Mock-transfected L929 cells and cells transfected with an empty plasmid or with a plasmid encoding hSCARB2-F or mScarb2-F were infected with EV71 at a low MOI. Viral titers in Vero cells were determined at 0, 24, and 48 h postinfection. The data are shown as mean viral titers with standard deviations (n = 3).

cells were detected in hSCARB2-F-transfected cells, whereas a modest number were detected in mScarb2-F-transfected cells (Fig. 3C). By FACS analysis, the number of GFP-positive cells was significantly greater in L929 cells expressing hSCARB2-F than in those expressing mScarb2-F ($P = 0.0032$) (Fig. 3D). These results indicate that EV71-GFP infected efficiently via hSCARB2 and less efficiently via mScarb2 and that the efficiencies of infection by use of the two receptors were significantly different.

Multistep EV71 infection of L929 cells expressing hSCARB2 and mScarb2. To validate the results obtained with the single-round infection experiment using EV71-GFP, we performed a multistep infection assay with wild-type EV71 infecting at a low multiplicity of infection (MOI) to examine the spread of the virus. We confirmed by immune staining and Western blotting that hSCARB2-F and mScarb2-F were transfected and expressed at similar levels (data not shown). L929 cells expressing hSCARB2-F and mScarb2-F were infected with EV71, and the viral titers were determined at each time point (Fig. 4). EV71 grew efficiently in L929 cells expressing hSCARB2-F but only moderately in L929 cells expressing mScarb2-F. At the last time point, the viral titer in L929 cells expressing hSCARB2-F was approximately 100-fold higher than that in L929 cells expressing mScarb2-F. EV71 propagated minimally in mock-transfected and empty-plasmid-transfected L929 cells. These results indicate that EV71 infected more efficiently via hSCARB2 than via mScarb2.

Binding of hSCARB2 and mScarb2 to EV71. To elucidate the functional difference between hSCARB2 and mScarb2 in the early steps of infection, we conducted pulldown assays to compare the binding affinities of soluble hSCARB2-Fc and soluble mScarb2-Fc for EV71 (Fig. 5A). EV71 was incubated with BSA, control Fc, hSCARB2-Fc, or mScarb2-Fc and with anti-Fc-agarose beads, and precipitated proteins were analyzed by Western blotting. EV71 VP1 was detected at all concentrations of hSCARB2-Fc, and the amount of precipitated VP1 increased in a concentration-dependent manner, as reported previously (37). However, while mScarb2-Fc was precipitated at a level similar to that of hSCARB2-Fc at each concentration

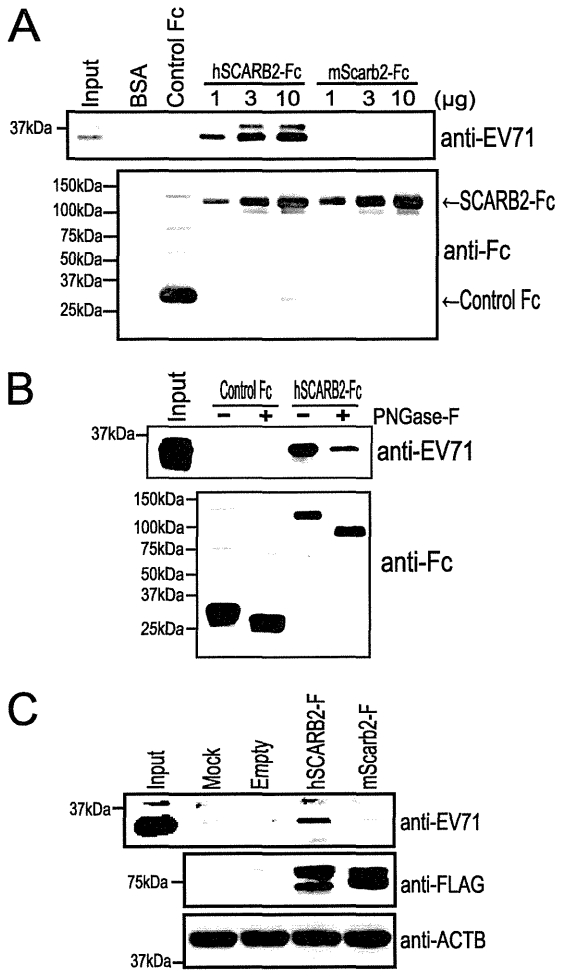

FIG. 5. Binding of hSCARB2 to EV71. (A) hSCARB2-Fc bound to EV71. A total of 10 μg of BSA, 10 μg of control Fc, or 1, 3, or 10 μg of hSCARB2-Fc or mScarb2-Fc was bound to anti-human Fc-agarose and was incubated with EV71. The precipitated proteins were analyzed by Western blotting with an anti-EV71 or anti-Fc antibody. The anti-EV71 antibody detected primarily the viral VP1 protein. (B) hSCARB2-Fc with or without N-linked carbohydrate chains bound to EV71. EV71 was incubated with 3 μg of control Fc or 3 μg of hSCARB2-Fc treated with PNGase F, and the proteins were precipitated with an anti-Fc antibody. The precipitated proteins were analyzed by Western blotting with an anti-EV71 or anti-Fc antibody. (C) EV71 attached to hSCARB2-expressing L929 cells. L929 cells were either mock transfected or transfected with an empty plasmid, pCA-hSCARB2-F, or pCA-mScarb2-F. The transfected cells were incubated with EV71 at 4°C. After the wash steps, the cells were lysed and analyzed by Western blotting with an anti-EV71, anti-FLAG, or anti-ACTB antibody. ACTB was used as a loading control.

(Fig. 5A, lower panel), VP1 was not detected at any concentration of mScarb2-Fc (Fig. 5A, upper panel). VP1 did not precipitate with BSA or control Fc. These data show that the binding affinity of hSCARB2 for EV71 was stronger than that of mScarb2.

To determine whether the N-linked carbohydrate chains of hSCARB2 contribute to the binding to virions, the native form of hSCARB2-Fc was treated with PNGase F. The removal of the carbohydrate chains from hSCARB2-Fc was confirmed by the 25-kDa downward size shift observed by Western blotting in the protein treated with PNGase F. PNGase F-treated hSCARB2-Fc or untreated hSCARB2-Fc was mixed with virions. After immunoprecipitation, bound virions and Fc proteins were analyzed by Western blotting (Fig. 5B). EV71 coprecipitated with both PNGase F-treated and nontreated hSCABR2-Fc; however, the intensity of the EV71 VP1 band coprecipitating with PNGase F-treated hSCARB2-Fc was only moderately lower than that of the band coprecipitating with nontreated hSCARB2-Fc. These results indicate that the carbohydrate chains of hSCARB2 are not essential for the EV71–hSCARB2 interaction.

To assess the binding of EV71 to SCARB2 at the plasma membrane, we performed virus attachment assays using a transient expression system (Fig. 5C). L929 cells were either mock transfected or transfected with an empty plasmid, pCA-hSCARB2-F, or pCA-mScarb2-F. The expression level of hSCARB2-F was similar to that of mScarb2-F (Fig. 5C, center). After 48 h posttransfection, these cells were mixed with EV71, washed to remove unbound virus, lysed together with bound viruses, and then analyzed by Western blotting. The amount of EV71 that was bound to cells transfected with pCA-hSCARB2 was substantially greater than that bound to mock-transfected cells or to cells transfected with an empty plasmid or pCA-mScarb2 (Fig. 5C, top). These data show that the binding affinity of EV71 for hSCARB2 in the membrane was stronger than that for mScarb2 in the membrane.

Determination of the hSCARB2 region that mediates EV71 infection. Because EV71 infected L929 cells more efficiently via hSCARB2 than via mScarb2 (Fig. 4), we mapped the region(s) that was important for EV71 infection by using chimeric hSCARB2–mScarb2 mutants. We hypothesized that the efficiency of EV71 infection via hSCARB2 would be lowered by replacement of the important region(s) with the corresponding region(s) in mScarb2 and vice versa. For this purpose, we prepared 6 chimeric mutants in which some of the exons were replaced (Fig. 6A). In the H(M1-4)-F mutant, for example, the human amino acid sequence 1 to 204, encoded in *hSCARB2* exons 1 to 4, was replaced with the corresponding region from mScarb2. Other chimeric mutants were constructed according to the same strategy. We performed the single-round infection assay to compare the efficiencies of EV71-GFP infection via these chimeras. All mutants were transfected and expressed at similar levels (Fig. 6B). Transfected cells were infected with EV71-GFP and were imaged with a microscope at 24 h postinfection (data not shown). These cells were analyzed by FACS to count the number of GFP-positive cells (Fig. 6C). Among the hSCARB2 backbone chimeric mutants, the H(M1-4)-F mutant failed to mediate efficient EV71-GFP infection. Among the mScarb2 backbone chimeras, the M(H1-4)-F mutant mediated efficient EV71-GFP infection. These data indicate that the region from amino acids 1 to 204, encoded in human *SCARB2* exons 1 to 4, is important for EV71-GFP infection.

To refine the region important for EV71-GFP infection, we constructed an additional 8 chimeric mutants in each of which one of exons 1 to 4 was replaced (Fig. 7A). The transfection efficiencies of all chimeric mutants were comparable (data not shown). Expression of chimeric mutants in L929 cells was confirmed by Western blotting (Fig. 7B). We found that the levels of expression of mutants H(M1)-F, H(M2)-F, H(M3)-F,

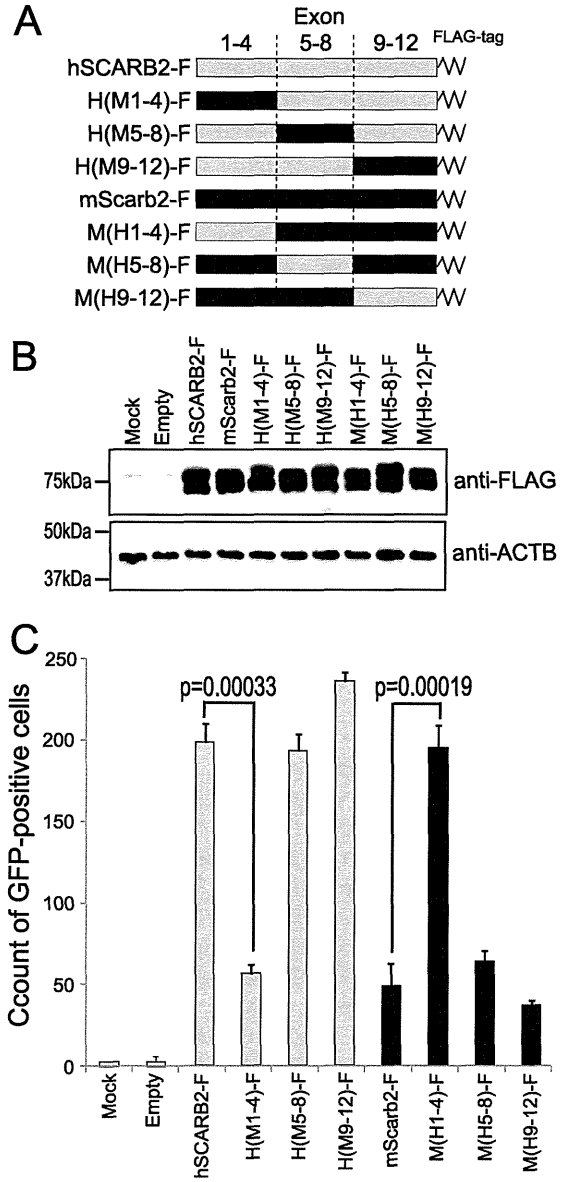

FIG. 6. Amino acids 1 to 204 of hSCARB2 are important for efficient EV71 infection. (A) Schematic diagram of chimeric hSCARB2–mScarb2 mutants. A series of mutants was constructed by the sequential substitution of a set of 4 exons. A FLAG tag was added at the C terminus of the open reading frame. (B and C) Single-round infection assays were performed to compare the efficiencies of EV71 infection as described in the legend to Fig. 3. FACS data are shown as mean counts with standard deviations (n = 3). Statistical significance was determined by Student's t test.

M(H1)-F, and M(H4)-F were comparable to that of hSCARB2-F, and the ratios of the two major molecular species migrating at approximately 80 kDa and 70 kDa were similar to that for hSCARB2-F. Two species of approximately 80 kDa and 70 kDa for H(M4)-F and M(H3)-F were detected; however, the intensity of the 80-kDa species in H(M4)-F and M(H3)-F was lower than that in hSCARB2. In M(H2)-F-transfected cells, we detected at least 3 species migrating at approximately 55 kDa, 80 kDa, and 90 kDa. Treatment of wild-type SCARB2-F and the three chimeric mutants with PNGase F resulted in similar apparent molecular masses (Fig. 7D). This result shows that the differences in the mobility and the ratios of these species between these three mutants were caused by differing N-glycosylation patterns and not by protein degradation. Replacement of a region in hSCARB2 with the corresponding region in mScarb2, and vice versa, may affect protein folding and it may contribute to the difference in N-glycosylation patterns. We performed the single-round infection assay to determine the infection efficiency. The transfected cells were infected with EV71-GFP and were analyzed by FACS to count the number of GFP-positive cells (Fig. 7C). In a series of experiments using the hSCARB2 backbone chimeras, the number of GFP-positive cells in cells expressing H(M4)-F was significantly decreased (P = 0.000039). In experiments using the mScarb2 backbone chimeras, the number of GFP-positive cells in cells expressing M(H4)-F was significantly greater (P = 0.00071). These data indicate that the region from amino acids 142 to 204, encoded in *SCARB2* exon 4, is important for EV71-GFP infection.

To further refine the region important for EV71 infection, we constructed 4 chimeric mutants in which the first or second half of exon 4 was replaced with the sequence of the other species of origin, and we analyzed infection efficiency with the single-round infection assay. Each mutant showed an infection efficiency intermediate between those of hSCARB2 and mScarb2 (data not shown). These data indicate that the important amino acids for EV71 infection are localized throughout the region from amino acids 142 to 204.

Multistep infection of L929 cells expressing H(M4)-F or M(H4)-F. In order to confirm the important region identified by the single-round infection assay, we carried out multistep infection assays to determine the spread of wild-type EV71 in chimera-expressing L929 cells. L929 cells were transfected with plasmids encoding hSCARB2-F, mScarb2-F, H(M4)-F, or M(H4)-F and were subsequently infected with EV71. Viral titers were determined at each time point (Fig. 8). EV71 grew as efficiently in L929 cells expressing M(H4)-F as in L929 cells expressing hSCARB2-F, whereas EV71 grew at a moderate level in L929 cells expressing M(H4)-F or mScarb2-F. The final viral titer in L929 cells expressing hSCARB2-F or M(H4)-F was approximately 40-fold higher than that in L929 cells expressing mScarb2-F or H(M4)-F. These results indicate that the M(H4)-F mutant functioned as a receptor for EV71 with an efficiency similar to that of hSCARB2-F.

Binding of H(M4)-F and M(H4)-F to EV71. Because the region from amino acids 142 to 204 was important for the single and multistep EV71 infections, we presumed that this region played a critical role in the binding of EV71. Before a virus attachment assay was performed, the expression of hSCARB2-F, mScarb2-F, H(M4)-F, and M(H4)-F on the cell surface was confirmed by biotinylation of cell surface proteins (Fig. 9A). Similar amounts of biotinylated hSCARB2-F, mScarb2-F, H(M4)-F, and M(H4)-F were precipitated with NeutrAvidin agarose resin. Without biotinylation, no FLAG-tagged receptors were precipitated. These results indicate that these receptors were expressed comparably at the cell surface. Next, L929 cells transfected with a plasmid encoding hSCARB2-F, mScarb2-F, H(M4)-F, or M(H4)-F were mixed with EV71, and bound viruses were detected by Western blotting. The amount of EV71 VP1 that bound to cells expressing

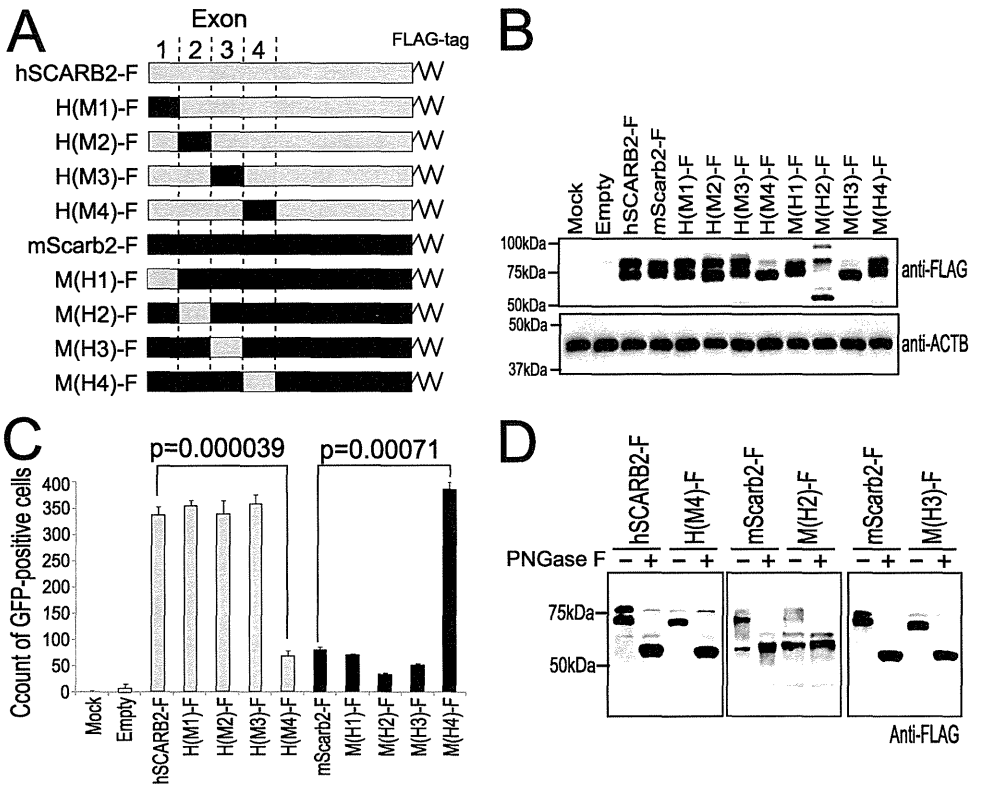

FIG. 7. The region from amino acids 142 to 204 of hSCARB2 is important for efficient EV71 infection. (A) Schematic diagram of chimeric hSCARB2–mScarb2 mutants. A series of mutants was constructed by the substitution of exons 1 to 4 individually. A FLAG tag was added at the C terminus of the open reading frame. (B and C) Single-round infection assays. (B) Expression of hSCARB2-F, mScarb2-F, and chimeric receptors was confirmed by Western blot analysis with an anti-FLAG antibody. ACTB was used as a loading control for the Western blot. (C) Transfected cells infected with EV71-GFP were analyzed by FACS. The FACS data are shown as mean counts with standard deviations (n = 3). Statistical significance was determined by Student's t test. (D) PNGase F treatment of H(M4)-F, M(H2)-F, and M(H3)-F. L929 cells were transfected with a plasmid encoding H(M4)-F, M(H2)-F, or M(H3)-F. The cells were treated with PNGase F, and the samples were analyzed by Western blotting with an anti-FLAG antibody.

hSCARB2-F or M(H4)-F was clearly larger than that for cells that were either mock transfected or transfected with an empty plasmid, mScarb2-F, or H(M4)-F. These results indicate that M(H4)-F bound to EV71 at a level similar to that of hSCARB2-F.

DISCUSSION

The viral receptor plays multiple roles, including the key steps for viral entry, viral attachment, possible internalization, and/or uncoating. We have shown that EV71 efficiently infected mouse cells via hSCARB2 but not via mScarb2. Using soluble receptors and receptor-expressing cells, we demonstrated that hSCARB2, but not mScarb2, bound efficiently to EV71. The binding of mScarb2 to EV71 was too weak to detect under our experimental conditions. We conclude that the ability of SCARB2 molecules to bind to EV71 virions is at least one of the major functional differences between hSCARB2 and mScarb2. Other receptor roles, such as internalization and uncoating, in the SCARB2 molecule require elucidation in further studies.

We have mapped the region of human SCARB2 that is important for both efficient virus binding and the establishment of infection to amino acids 142 to 204 by using human SCARB2 and mouse Scarb2 chimeric receptors. The overall amino acid identity between hSCARB2 and mScarb2 was 85.8%, while the local amino acid identity of amino acids 142 to 204 was 76.2%. EV71 binds a region that is divergent for the human and mouse sequences. Amino acids 142 to 204 may form the core region of the binding site for virions. We prepared a fusion protein consisting of amino acids 142 to 204 of hSCARB2 and the Fc region of human IgG (H4-Fc) in order to determine whether this region was sufficient for virus binding. However, an attempt to precipitate EV71 with H4-Fc was not successful (data not shown). This failure suggested two possibilities: either that that H4 region, which would have been sufficient for virus binding, was not folded appropriately in the fusion protein or that some amino acids outside this region, which are common to the human and mouse sequences, participate in the interaction. Recently, it was reported that a coiled-coil domain of SCARB2/LIMPII at positions 152 to 167, which included the region important for EV71 infection and binding, is necessary for β-GC binding (5). This report indicates that the region from amino acids 142 to 204 is potentially exposed on the surface of the protein.

There is no potential N-glycosylation site in the region from amino acids 142 to 204 of hSCARB2 or mScarb2. Moreover, we showed that the N-linked carbohydrate chains of hSCARB2

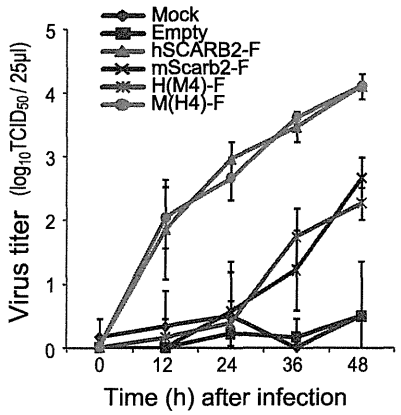

FIG. 8. Multistep infections of EV71. Mock-transfected L929 cells and cells transfected with an empty plasmid or a plasmid encoding hSCARB2-F, mScarb2-F, H(M4)-F, or M(H4)-F were infected with EV71 at a low MOI. Viral titers in Vero cells were determined at 0, 12, 24, 36, and 48 h postinfection. The data are shown as mean viral titers with standard deviations (n = 3).

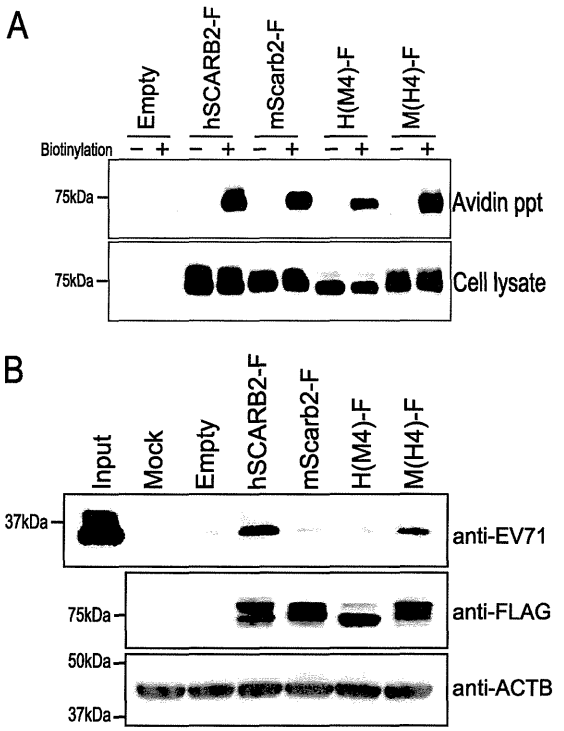

FIG. 9. The M(H4)-F mutant bound to EV71 as efficiently as hSCARB2-F. (A) Biotinylation of cell surface proteins. L929 cells were transfected with an empty plasmid, pCA-hSCARB2-F, pCA-mScarb2-F, pCA-H(M4)-F, or pCA-M(H4)-F. Cell surface proteins of transfected cells were biotinylated and precipitated with NeutrAvidin agarose resin. Precipitated proteins (Avidin ppt) and total-cell lysates (Cell lysate) were analyzed by Western blotting with the anti-FLAG antibody. (B) Binding of EV71 to chimeras. L929 cells were either mock transfected or transfected with an empty plasmid, pCA-hSCARB2-F, pCA-mScarb2-F, pCA-H(M4)-F, or pCA-M(H4)-F. These cells were incubated with EV71 at 4°C. After the wash steps, the cells and bound viruses were lysed and analyzed by Western blotting with an anti-EV71 or anti-FLAG antibody. ACTB was used as a loading control.

were not essential for the EV71–hSCARB2 interaction. Taken together, the results suggest that direct protein-protein interaction is essential for the EV71–SCARB2 interaction. However, in immunoprecipitation experiments using soluble hSCARB2-Fc, hSCARB2-Fc treated with PNGase F coprecipitated reduced amounts of EV71. Therefore, we cannot exclude the possibility that N-linked carbohydrate chains play some role in the binding of hSCARB2 to EV71, such as bridging of the EV71–hSCARB2 interaction or stabilization of the conformation of hSCARB2.

Several types of picornavirus receptors have been identified and characterized. Each type of receptor has characteristics common to the family. Receptors of the first type, which include poliovirus receptor (PVR), intercellular adhesion molecule 1 (ICAM-1) of major group rhinoviruses, human coxsackievirus B and adenovirus 2 receptor (HCAR) of coxsackievirus B1 to B6, and vascular cell adhesion molecule 1 (VCAM-1) of encephalomyocarditis virus (EMCV), are members of the immunoglobulin superfamily whose extracellular regions have two to seven Ig-like domains (9, 15, 18, 20). These type II transmembrane receptors sterically bind to the virus canyon at the distal Ig-like domain (D1) through multiple amino acids (22, 34). Receptors of the second type, the $\alpha_v\beta_1$, $\alpha_v\beta_3$, and $\alpha_v\beta_6$ integrins of parechovirus, cocsackievirus A9, and foot-and-mouth disease virus (FMDV), belong to the integrin family and bind to an exposed RGD motif on the virion surface via their α or β chain (7, 34, 35, 38). Receptors of the third type, which include low-density lipoprotein receptor (LDL-R) of minor group rhinoviruses and decay-accelerating factor (DAF) of some echoviruses and group B coxsackieviruses, bind outside the canyon via complement type A repeats and short consensus repeats (SCRs), respectively (4, 9, 16). Although SCARB2 does not belong to the immunoglobulin superfamily or the integrin family, we identified the region (amino acids 142 to 204) of hSCARB2 that mediates viral attachment and infection. In this region, multiple amino acids spanning the entire region from 142 to 204 are important for binding and infection. Similar results have been shown for the D1 region of PVR. Three main sites have been found to be important for poliovirus binding: (i) the C-C′ loop through the C″ strand, (ii) the border of the D strand and the D-E loop, and (iii) the G strand (2, 3, 15, 24, 29). Therefore, hSCARB2 binds to EV71 with multiple contact points, which suggests that the region spanning amino acids 142 to 204 of hSCARB2 may bind to the viral canyon in a manner similar to the interaction between poliovirus and PVR. The crystallization of the EV71 virions and SCARB2 or the cocrystallization of EV71 with SCARB2 should reveal the EV71–SCARB2 interaction at the atomic level. The identification of the region in hSCARB2 that mediates binding and infection would bring new insight into the nature of the virus-receptor interaction of picornaviruses, and further studies would contribute to a thorough understanding of the binding of EV71 to the receptor.

In summary, our data have shown that amino acids 142 to 204 (encoded in human *SCARB2* exon 4) of SCARB2 are important for EV71 infection and binding. The identification of this region of human SCARB2 that is required for the EV71 infection greatly contributes to the understanding of virus-receptor interactions, because human SCARB2 has no known

picornavirus receptor motifs. Further studies would clarify the early steps of EV71 infection. The replacement of exon 4 of mouse *Scarb2* with the corresponding human SCARB2 sequence will lead to the development of a new mouse model susceptible to EV71. These mice will greatly contribute to the understanding of EV71 neuropathogenicity *in vivo* and possibly to the development of a vaccine and/or an antiviral drug.

ACKNOWLEDGMENTS

We thank H. Shimizu and Y. Nishimura (NIDD of Japan) for providing us with EV71 strain SK-EV006/Malaysia/97 and for helpful discussions, Y. Kawaoka (University of Tokyo) for providing us with pCAGGS.MCS, and K. Fujii for useful discussions and critical reading of the manuscript.

This work was supported in part by a Grant-in-Aid for Scientific Research (C) (20590243) from the Japan Society for the Promotion of Science, in part by a Grant-in-Aid for Young Scientists (B) (21790454) from the Ministry of Education, Culture, Sports, Science and Technology (MEXT), and in part by a Grant-in-Aid for Research on Emerging and Re-emerging Infectious Diseases from the Ministry of Health, Labor and Welfare of Japan.

REFERENCES

1. **Ahmad, K.** 2000. Hand, foot, and mouth disease outbreak reported in Singapore. Lancet **356:**1338.
2. **Aoki, J., S. Koike, I. Ise, Y. Sato-Yoshida, and A. Nomoto.** 1994. Amino acid residues on human poliovirus receptor involved in interaction with poliovirus. J. Biol. Chem. **269:**8431–8438.
3. **Belnap, D. M., et al.** 2000. Three-dimensional structure of poliovirus receptor bound to poliovirus. Proc. Natl. Acad. Sci. U. S. A. **97:**73–78.
4. **Bergelson, J. M., et al.** 1994. Decay-accelerating factor (CD55), a glycosylphosphatidylinositol-anchored complement regulatory protein, is a receptor for several echoviruses. Proc. Natl. Acad. Sci. U. S. A. **91:**6245–6248.
5. **Blanz, J., et al.** 2010. Disease-causing mutations within the lysosomal integral membrane protein type 2 (LIMP-2) reveal the nature of binding to its ligand beta-glucocerebrosidase. Hum. Mol. Genet. **19:**563–572.
6. **Blomberg, J., et al.** 1974. New enterovirus type associated with epidemic of aseptic meningitis and-or hand, foot, and mouth disease. Lancet **ii:**112. (Letter.)
7. **Burman, A., et al.** 2006. Specificity of the VP1 GH loop of foot-and-mouth disease virus for αv integrins. J. Virol. **80:**9798–9810.
8. **Chan, L. G., et al.** 2000. Deaths of children during an outbreak of hand, foot, and mouth disease in Sarawak, Malaysia: clinical and pathological characteristics of the disease. For the Outbreak Study Group. Clin. Infect. Dis. **31:**678–683.
9. **Coyne, C. B., and J. M. Bergelson.** 2006. Virus-induced Abl and Fyn kinase signals permit coxsackievirus entry through epithelial tight junctions. Cell **124:**119–131.
10. **Eskelinen, E. L., Y. Tanaka, and P. Saftig.** 2003. At the acidic edge: emerging functions for lysosomal membrane proteins. Trends Cell Biol. **13:**137–145.
11. **Fujimoto, T., et al.** 2002. Outbreak of central nervous system disease associated with hand, foot, and mouth disease in Japan during the summer of 2000: detection and molecular epidemiology of enterovirus 71. Microbiol. Immunol. **46:**621–627.
12. **Gamp, A. C., et al.** 2003. LIMP-2/LGP85 deficiency causes ureteric pelvic junction obstruction, deafness and peripheral neuropathy in mice. Hum. Mol. Genet. **12:**631–646.
13. **Hagiwara, A., I. Tagaya, and T. Yoneyama.** 1978. Epidemic of hand, foot and mouth disease associated with enterovirus 71 infection. Intervirology **9:**60–63.
14. **Hatakeyama, S., et al.** 2005. Enhanced expression of an α2,6-linked sialic acid on MDCK cells improves isolation of human influenza viruses and evaluation of their sensitivity to a neuraminidase inhibitor. J. Clin. Microbiol. **43:**4139–4146.
15. **He, Y., et al.** 2000. Interaction of the poliovirus receptor with poliovirus. Proc. Natl. Acad. Sci. U. S. A. **97:**79–84.
16. **Hewat, E. A., et al.** 2000. The cellular receptor to human rhinovirus 2 binds around the 5-fold axis and not in the canyon: a structural view. EMBO J. **19:**6317–6325.
17. **Ho, M., et al.** 1999. An epidemic of enterovirus 71 infection in Taiwan. Taiwan Enterovirus Epidemic Working Group. N. Engl. J. Med. **341:**929–935.
18. **Huber, S. A.** 1994. VCAM-1 is a receptor for encephalomyocarditis virus on murine vascular endothelial cells. J. Virol. **68:**3453–3458.
19. **Kobasa, D., M. E. Rodgers, K. Wells, and Y. Kawaoka.** 1997. Neuraminidase hemadsorption activity, conserved in avian influenza A viruses, does not influence viral replication in ducks. J. Virol. **71:**6706–6713.
20. **Kolatkar, P. R., et al.** 1999. Structural studies of two rhinovirus serotypes complexed with fragments of their cellular receptor. EMBO J. **18:**6249–6259.
21. **Kuronita, T., et al.** 2002. A role for the lysosomal membrane protein LGP85 in the biogenesis and maintenance of endosomal and lysosomal morphology. J. Cell Sci. **115:**4117–4131.
22. **Lin, J. Y., et al.** 2009. Viral and host proteins involved in picornavirus life cycle. J. Biomed. Sci. **16:**103.
23. **McMinn, P. C.** 2002. An overview of the evolution of enterovirus 71 and its clinical and public health significance. FEMS Microbiol. Rev. **26:**91–107.
24. **Morrison, M. E., Y. J. He, M. W. Wien, J. M. Hogle, and V. R. Racaniello.** 1994. Homolog-scanning mutagenesis reveals poliovirus receptor residues important for virus binding and replication. J. Virol. **68:**2578–2588.
25. **Nagata, N., et al.** 2002. Pyramidal and extrapyramidal involvement in experimental infection of cynomolgus monkeys with enterovirus 71. J. Med. Virol. **67:**207–216.
26. **Nishimura, Y., et al.** 2009. Human P-selectin glycoprotein ligand-1 is a functional receptor for enterovirus 71. Nat. Med. **15:**794–797.
27. **Qiu, J.** 2008. Enterovirus 71 infection: a new threat to global public health? Lancet Neurol. **7:**868–869.
28. **Racaniello, V.** 2007. Picornaviridae: the viruses and their replication, p. 795–838. *In* D. M. Knipe, P. M. Howley, D. E. Griffin, R. A. Lamb, M. A. Martin, B. Roizman, and S. E. Straus (ed.), Fields virology, 5th ed. Lippincott Williams & Wilkins, Philadelphia, PA.
29. **Racaniello, V. R.** 1996. Early events in poliovirus infection: virus-receptor interactions. Proc. Natl. Acad. Sci. U. S. A. **93:**11378–11381.
30. **Reczek, D., et al.** 2007. LIMP-2 is a receptor for lysosomal mannose-6-phosphate-independent targeting of beta-glucocerebrosidase. Cell **131:**770–783.
31. **Reed, L. J., and H. Muench.** 1938. A simple method of estimating 50 percent endpoints. Am. J. Hyg. (Lond.) **27:**493–497.
32. **Rossmann, M. G., and J. E. Johnson.** 1989. Icosahedral RNA virus structure. Annu. Rev. Biochem. **58:**533–573.
33. **Schmidt, N. J., E. H. Lennette, and H. H. Ho.** 1974. An apparently new enterovirus isolated from patients with disease of the central nervous system. J. Infect. Dis. **129:**304–309.
34. **Semler, B., and E. Wimmer.** 2002. Molecular biology of picornaviruses. ASM Press, Washington, DC.
35. **Williams, C. H., et al.** 2004. Integrin $\alpha_v\beta_6$ is an RGD-dependent receptor for coxsackievirus A9. J. Virol. **78:**6967–6973.
36. **Yamayoshi, S., et al.** 2008. Ebola virus matrix protein VP40 uses the COPII transport system for its intracellular transport. Cell Host Microbe **3:**168–177.
37. **Yamayoshi, S., et al.** 2009. Scavenger receptor B2 is a cellular receptor for enterovirus 71. Nat. Med. **15:**798–801.
38. **Yan, J. J., J. R. Wang, C. C. Liu, H. B. Yang, and I. J. Su.** 2000. An outbreak of enterovirus 71 infection in Taiwan 1998: a comprehensive pathological, virological, and molecular study on a case of fulminant encephalitis. J. Clin. Virol. **17:**13–22.
39. **Yang, B., H. Chuang, and K. D. Yang.** 2009. Sialylated glycans as receptor and inhibitor of enterovirus 71 infection to DLD-1 intestinal cells. Virol. J. **6:**141.
40. **Yang, F., et al.** 2009. Enterovirus 71 outbreak in the People's Republic of China in 2008. J. Clin. Microbiol. **47:**2351–2352.

References

1. Deguchi T, Maeda S. *Mycoplasma genitalium*: another important pathogen of nongonococcal urethritis. J Urol. 2002;167:1210–7. doi:10.1016/S0022-5347(05)65268-8
2. Jensen JS. *Mycoplasma genitalium*: the aetiological agent of urethritis and other sexually transmitted diseases. J Eur Acad Dermatol Venereol. 2004;18:1–11. doi:10.1111/j.1468-3083.2004.00923.x
3. Mena LA, Mroczkowski TF, Nsuami M, Martin DH. A randomized comparison of azithromycin and doxycycline for the treatment of *Mycoplasma genitalium*–positive urethritis in men. Clin Infect Dis. 2009;48:1649–54. doi:10.1086/599033
4. Bradshaw CS, Jensen JS, Tabrizi SN, Read TR, Garland SM, Hopkins CA, et al. Azithromycin failure in *Mycoplasma genitalium* urethritis. Emerg Infect Dis. 2006;12:1149–52.
5. Jensen JS, Bradshaw CS, Tabrizi SN, Fairley CK, Hamasuna R. Azithromycin treatment failure in *Mycoplasma genitalium*–positive patients with nongonococcal urethritis is associated with induced macrolide resistance. Clin Infect Dis. 2008;47:1546–53. doi:10.1086/593188
6. Jensen JS, Hansen HT, Lind K. Isolation of *Mycoplasma genitalium* strains from the male urethra. J Clin Microbiol. 1996;34:286–91.
7. Hamasuna R, Osada Y, Jensen JS. Antibiotic susceptibility testing of *Mycoplasma genitalium* by TaqMan 5′ nuclease real-time PCR. Antimicrob Agents Chemother. 2005;49:4993–8. doi:10.1128/AAC.49.12.4993-4998.2005
8. Hamasuna R, Jensen JS, Osada Y. Antimicrobial susceptibilities of *Mycoplasma genitalium* strains examined by broth dilution and quantitative PCR. Antimicrob Agents Chemother. 2009;53:4938–9.
9. Vester B, Douthwaite S. Macrolide resistance conferred by base substitutions in 23S rRNA. Antimicrob Agents Chemother. 2001;45:1–12. doi:10.1128/AAC.45.1.1-12.2001
10. Diner EJ, Hayes CS. Recombineering reveals a diverse collection of ribosomal proteins L4 and L22 that confer resistance to macrolide antibiotics. J Mol Biol. 2009;386:300–15. doi:10.1016/j.jmb.2008.12.064

Address for correspondence: Takashi Deguchi, Department of Urology, Graduate School of Medicine, Gifu University, 1-1 Yanagido, Gifu City, Gifu 501-1194, Japan; email: deguchit@gifu-u.ac.jp

Saffold Cardioviruses in Children with Diarrhea, Thailand

To the Editor: Cardioviruses currently consist of at least 3 viruses: Theiler murine encephalomyocarditis virus, encephalomyocarditis virus, and Saffold virus (SAFV) (*1–4*). Saffold cardiovirus in the family *Picornaviridae* was isolated and identified from fecal specimens of a child with fever of unknown origin in the United States (*3*).

Several reports have documented the presence of SAFV in fecal samples and respiratory secretions (*5–10*). However, it is not clear whether SAFV is associated with any disease, including gastroenteritis in humans, and epidemiologic data for SAFV are limited. We report an epidemiologic survey of SAFV in children hospitalized with diarrhea in Chiang Mai, Thailand.

A total of 150 fecal specimens were obtained from children hospitalized with acute gastroenteritis in Chiang Mai during January–December 2007. Patient ages ranged from >1 to 5 years. SAFV in fecal specimens was detected by using a nested PCR and primers specific for the virus 5′ untranslated region (*7*). A negative control was also included to monitor any contamination that might have occurred during the PCR.

SAFVs detected were further analyzed by amplification of the viral protein (VP) 1 gene (*6,9,10*) and direct sequencing of the VP1 PCR amplicon by using the BigDye Terminator Cycle Sequencing Kit (Applied Biosystems, Foster City, CA, USA). VP1 sequence was compared with VP1 sequences of reference strains available in the National Center for Biotechnology Information (Bethesda, MD, USA). Phylogenetic and molecular evolutionary analyses were conducted by using MEGA4 (www.megasoftware.net). Nucleotide sequences of SAFV strains described were deposited in GenBank under accession nos. HQ668170–HQ668173.

Four (2.7%) of 150 specimens were positive for SAFV (CMH023/2007, CMH038/2007, CMH045/2007, and CMH143/2007). Two of these specimens (CMH023/2007 and CMH038/2007) were obtained in February 2007, one (CMH045/2007) in March 2007, and 1 (CMH143/2007) in November 2007. Co-infections with other viruses were detected in all 4 samples. Two specimens (CMH023/2007and CMH045/2007), were co-infected with noroviruses GII/16 and GII/4 genotypes, respectively. One SAFV-positive sample (CMH038/2007) was co-infected with a group A rotavirus G1P[8] genotype, and another (CMH143/2007) was co-infected with human parechovirus.

All SAFV-positive specimens were further amplified for the VP1 gene to determine their phylogenetic lineages and genetic relationships with other SAFV reference strains. When we used 3 sets of primers used in other studies (*6,9,10*) for amplification of the VP1 gene, this gene was amplified only by the primer set reported by Itagaki et al. (*10*).

Analysis of partial VP1 sequences (369 nt) of 4 SAFV strains showed that strains CMH023/2007 and CMH143/2007 were highly conserved (nt sequence identities >97%). These 2 SAFV strains were most closely related to the prototype strain of SAFV1 (EF165067) isolated in the United States (nt sequence identity range 87.6%–88.9%) and SAFV strains from China (LZ50419, BCH895, GL311, and GL377) (Figure). In addition, the other 2 SAFVs identified in the present study (CMH038/2007 and CMH045/2007) were identical to each other and closely related to SAFV2 strains from China (BCHU79, BCHU353)

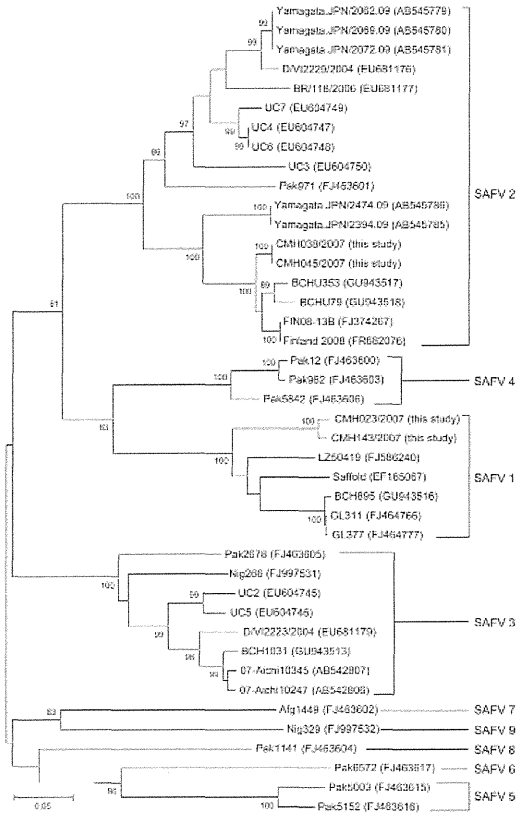

Figure. Phylogenetic analysis of the partial nucleotide sequence (369 nt) encoding the viral protein 1 gene of Saffold virus (SAFV) isolated in this study and other reference strains. The tree was generated by using the neighbor-joining method and MEGA4 (www.megasoftware.net). Bootstrap values >80 are indicated for the corresponding nodes on the basis of a resampling analysis of 1,000 replicates. Scale bar indicates nucleotide substitutions per site.

and Finland (Finland 2008, FIN08–13B) (nt sequence identity range 94.8%–95.6%). Phylogenetic analysis showed that CMH038/2007 and CMH045/2007 were clustered within the SAFV2 lineage (Figure).

The 4 strains of SAFV were isolated from children with acute gastroenteritis who were co-infected with other viral pathogens (norovirus, group A rotavirus, and human parechovirus). Therefore, we could not determine whether SAFVs identified in this study were associated with acute gastroenteritis. The detection rate for SAFV in children with acute gastroenteritis (2.7%) in our study was consistent with that in a study in Beijing, People's Republic of China (3.2%) (*9*).

Phylogenetic analysis of the VP1 region demonstrated that 2 SAFV lineages (SAFV1 and SAFV2) were circulating in Chiang Mai, Thailand. Further extensive epidemiologic surveillance of SAFV in other areas may provide a better understanding of the distribution, heterogeneity, and association of SAFV with enteric diseases in humans.

This study was supported by the Endowment Fund for Medical Research, Faculty of Medicine, Chiang Mai University, Thailand, and in part by Grants-in-Aid from the Ministry of Education and Sciences and the Ministry of Health, Labor and Welfare, Japan.

Pattara Khamrin, Natthawan Chaimongkol, Nattika Nantachit, Shoko Okitsu, Hiroshi Ushijima, and Niwat Maneekarn

Author affiliations: Chiang Mai University, Chiang Mai, Thailand (P. Khamrin, N. Chaimongkol, N. Maneekarn); Mahidol University, Bangkok, Thailand (N. Nantachit); and Nihon University School of Medicine, Tokyo, Japan (S. Okitsu, H. Ushijima)

DOI: 10.3201/eid1706.101983

References

1. LaRue R, Myers S, Brewer L, Shaw DP, Brown C, Seal BS, et al. A wild-type porcine encephalomyocarditis virus containing a short poly(C) tract is pathogenic to mice, pigs, and cynomolgus macaques. J Virol. 2003;77:9136–46. doi:10.1128/JVI.77.17.9136-9146.2003
2. Liang Z, Kumar AS, Jones MS, Knowles NJ, Lipton HL. Phylogenetic analysis of the species *Theilovirus*: emerging murine and human pathogens. J Virol. 2008;82:11545–54. doi:10.1128/JVI.01160-08
3. Jones MS, Lukashov VV, Ganac RD, Schnurr DP. Discovery of a novel human picornavirus in a stool sample from a pediatric patient presenting with fever of unknown origin. J Clin Microbiol. 2007;45:2144–50. doi:10.1128/JCM.00174-07
4. Drexler JF, Baumgarte S, Luna LK, Stöcker A, Almeida PS, Ribeiro TC, et al. Genomic features and evolutionary constraints in Saffold-like cardioviruses. J Gen Virol. 2010;91:1418–27. doi:10.1099/vir.0.018887-0
5. Abed Y, Boivin G. New Saffold cardioviruses in 3 children, Canada. Emerg Infect Dis. 2008;14:834–6.
6. Chiu CY, Greninger AL, Kanada K, Kwok T, Fischer KF, Runckel C, et al. Identification of cardioviruses related to Theiler's murine encephalomyelitis virus in human infections. Proc Natl Acad Sci U S A. 2008;105:14124–9. doi:10.1073/pnas.0805968105
7. Drexler JF, Luna LK, Stöcker A, Almeida PS, Ribeiro TC, Petersen N, et al. Circulation of 3 lineages of a novel Saffold cardiovirus in humans. Emerg Infect Dis. 2008;14:1398–405. doi:10.3201/eid1409.080570
8. Blinkova O, Kapoor A, Victoria J, Jones M, Wolfe N, Naeem A, et al. Cardioviruses are genetically diverse and cause common enteric infections in South Asian children.

J Virol. 2009;83:4631–41. doi:10.1128/JVI.02085-08
9. Ren L, Gonzalez R, Xiao Y, Xu X, Chen L, Vernet G, et al. Saffold cardiovirus in children with acute gastroenteritis, Beijing, China. Emerg Infect Dis. 2009;15:1509–11. doi:10.3201/eid1509.081531
10. Itagaki T, Abiko C, Ikeda T, Aoki Y, Seto J, Mizuta K, et al. Sequence and phylogenetic analyses of Saffold cardiovirus from children with exudative tonsillitis in Yamagata, Japan. Scand J Infect Dis. 2010;42:950–2. doi:10.3109/00365548.2010.496791

Address for correspondence: Niwat Maneekarn, Department of Microbiology, Faculty of Medicine, Chiang Mai University, Chiang Mai 50200, Thailand; email: nmaneeka@med.cmu.ac.th

Lethal Necrotizing Pneumonia Caused by an ST398 *Staphylococcus aureus* Strain

To the Editor: The prevalent colonization of livestock with methicillin-resistant *Staphylococcus aureus* (MRSA) sequence type (ST) 398 in many countries is a cause for consternation. However, understanding of the emergence of these organisms and their public health implications is embryonic. The perceptions that all MRSA found in livestock are of ST398 lineage or that livestock are the only reservoirs of ST398 oversimplify a complex epidemiology, therefore, prudence is required when attributing human infections with *S. aureus* ST398 to livestock reservoirs. The fatal infection of a young girl with ST398 methicillin-susceptible *S. aureus* (MSSA) is tragic (*1*). However, the conclusion by the authors that "the spread of *S. aureus* ST398 among livestock is a matter of increasing concern because strains of this sequence type were able to acquire PVL [Panton-Valentine leukocidin] genes" is misleading.

The authors report no history of livestock exposure and the *spa* type reported (t571) is relatively rare among livestock isolates (*2,3*). The isolate from the fatal case was tetracycline-susceptible and positive for PVL toxin, while livestock ST398 isolates have been almost uniformly tetracycline resistant and PVL negative. Notably, *spa* type t571 ST398 MSSA was detected in 9 families from the Dominican Republic living in Manhattan, New York, without contact with livestock (*4*). Furthermore, t571 was the only *spa* type of MSSA identified in a study in the Netherlands of ST398 isolates, including 3 independent cases of nosocomial bacteremia in Rotterdam with no apparent livestock contact (*5*). *spa* type t571 was the predominant (11%) MSSA type in patients at a Beijing, China, hospital (*6*). More recently, a study of t571 MSSA strains from cases of bloodstream infections in France determined that the isolates differed from pig-borne strains and shared similarities with strains from humans in China and virulent USA300 strains (*7*). These observations concur with a hypothesis that ST398 strains of diverse genotype and geographic origin may also be epidemiologically distinct (*8*), and livestock contact is a notably inconsistent feature of invasive ST398 infections (*5,7–10*).

The possibility that variants of the ST398 lineage may persist in human populations without livestock contact should not be dismissed. The incidence and severity of clinical infections with ST398 *S. aureus* in livestock workers as yet have been minimal. Understanding the public health implications of ST398 *S. aureus* requires systematic investigation of their epidemiology in animals and humans. Human clinical cases of ST398 *S. aureus* infection should not be indiscriminately attributed to livestock, particularly if isolates are genotypically dissimilar to those occurring commonly in animals.

Peter R. Davies, Elizabeth A. Wagstrom, and Jeffrey B. Bender

Author affiliation: University of Minnesota, St. Paul, Minnesota, USA

DOI: 10.3201/eid1706.101394

References

1. Rasigade J-P, Laurent F, Hubert P, Vandenesch F, Etienne J. Lethal necrotizing pneumonia caused by an ST398 *Staphylococcus aureus* strain. Emerg Infect Dis. 2010;16:1330.
2. de Neeling AJ, van den Broek MJ, Spalburg EC, van Santen-Verheuvel MG, Dam-Deisz WD, Boshuizen HC, et al. High prevalence of methicillin resistant *Staphylococcus aureus* in pigs. Vet Microbiol. 2007;122:366–72. doi:10.1016/j.vetmic.2007.01.027
3. Graveland H, Wagenaar JA, Heesterbeek H, Mevius D, van Duikeren E, Heedrik D. Methicillin resistant *Staphylococcus aureus* ST398 in veal calf farming: human MRSA carriage related with animal antimicrobial usage and farm hygiene. PLoS ONE. 2010;5:e10990. doi:10.1371/journal.pone.0010990
4. Bhat M, Dumortier C, Taylor B, Miller M, Vasquez G, Yunen J, et al. *Staphylococcus aureus* ST398, New York City and Dominican Republic. Emerg Infect Dis. 2009;15:285–7.
5. van Belkum A, Melles DC, Peeters JK, van Leeuwen WB, van Duijkeren E, Huijsdens XW, et al. Methicillin-resistant and -susceptible *Staphylococcus aureus* sequence type 398 in pigs and humans. Emerg Infect Dis. 2008;14:479–83. doi:10.3201/eid1403.0760
6. Chen H, Liu Y, Jiang X, Chen M, Wang H. Rapid change of methicillin-resistant *Staphylococcus aureus* clones in a Chinese tertiary care hospital over a 15-year period. Antimicrob Agents Chemother. 2010;54:1842–7. doi:10.1128/AAC.01563-09
7. van der Mee-Marquet N, François P, Domelier-Valentin AS, Coulomb F, Decreux C, Hombrock-Allet C, et al. Emergence of unusual bloodstream infections associated with pig-borne-like *Staphylococcus aureus* ST398 in France. Clin Infect Dis. 2011;52:152–3. doi:10.1093/cid/ciq053